SEA-ICE-OPTICS AND ROV-OPERATIONS DURING ARKXXVII/3 - ICEARC 2012

EXTENDED-CRUISE-REPORT

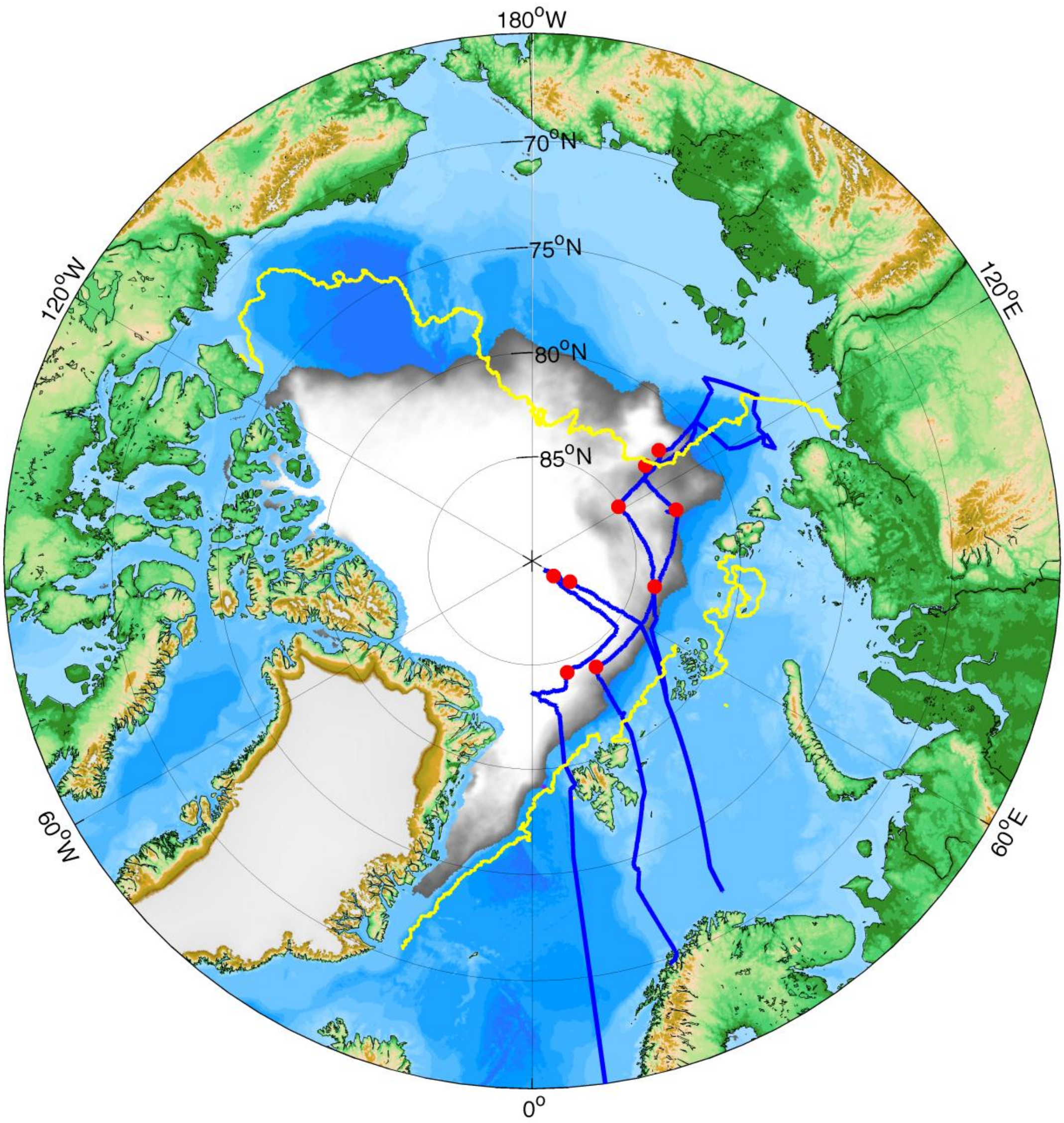

Christian Katlein[a], Marcel Nicolaus[a], Martin Schiller[a], Larysa Istomina[b], Scott Sörensen[c], Stefan Hendricks[a], Thomas Krumpen[a], Ben Lange[a]

[a] Alfred Wegener Institute, Bremerhaven
[b] Institute for Environmental Physics, Bremen
[c] University of Delaware

TABLE OF CONTENTS

INTRODUCTION

This cruise report is extending the report about the sea-ice work related to optical properties of sea-ice given in the official cruise report for RV Polarstern. Space was limited in the official report, so we present a detailed field report that focuses on the work itself. Details about the motivation and scientific questions addressed by this work can be found in the cruise booklet (Fahrbach and Knust 2012) and the official cruise report (Boetius 2012).

Following the successful examination of the optical properties of sea-ice during the TransArc Expedition 2012 (Schauer 2012), we continued our program of optical measurements under Arctic sea ice on this expedition. Compared to the year before we were able to improve our equipment to continue the comprehensive dataset obtained in the previous year.

CRUISE-TRACK

The expedition started on the 2nd of August in Tromsø. We entered the sea ice north of Franz-Joseph-land, where we had our first ice station and deployed the long-term station. The next ice-stations were placed along the east-going cruise-track. After a short excursion to the ice-free Laptev-sea we reentered the ice poleward. An accident during a safety drill forced us to return a patient to Kirkenes, before we could reenter the ice along the 60°E transect. After two successful icestations in the central pack ice close to the pole we returned south to retrieve our long-term-station before returning to Bremerhaven.

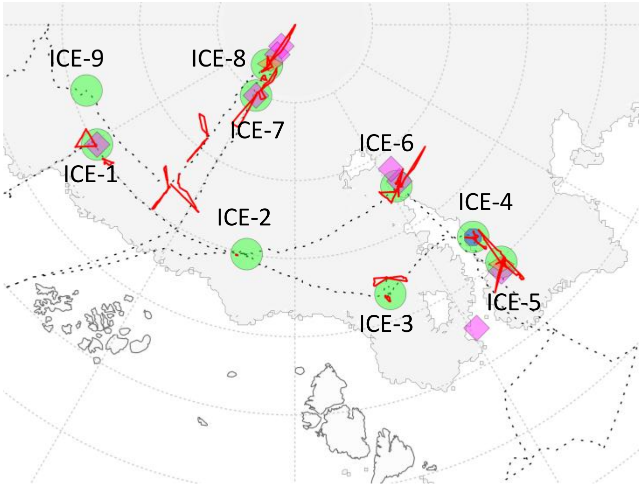

Figure 1: Cruise track of ARC-27/3, green circles highlight ice stations with indicated numbers. Sea ice extent from the beginning of the cruise is shown in light gray.

ICE-CONDITIONS

In the first part of the cruise we encountered very rotten and weak sea ice allowing for high steaming speeds. In some regions the freeboard had become extremely small, indicating very late melt stages. From above and underneath we observed huge channels in the ice, as melting had widened some brine channels up to a few decimeters. These conditions made it difficult to find floes stable enough to withstand the ships forces during the course of the regularly 72 hour long ice-stations.

In the central region close to the pole we observed harder ice-conditions, slowing down cruising speeds to less than 2 knots, mostly caused by the snow cover and refreezing conditions. Due to time limitations we were not able to reach the north-pole, but had to return about 134km before the pole. All ice observations are available from http://doi.pangaea.de/10.1594/PANGAEA.803221.

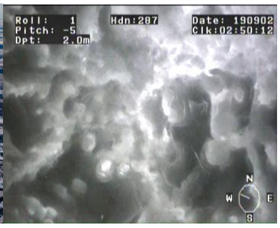

Figure 2: Aerial Image of very rotten first year ice observed during a helicopter flight (left); Melt structures of very rotten sea-ice as observed from the upward-looking ROV-camera during a ROV-survey (right).

ROV-SURVEYS

Operation of the ROV for light measurements during IceArc under the sea ice has been described previously (Katlein 2012, Nicolaus and Katlein 2012, Schauer 2012). Here we will mostly focus on the novelties of the IceArc system and the measurements made

THE ROV-SYSTEM

We used a rented Ocean Modules *V8Sii* observation class ROV (Ocean Modules, Åtvidaberg, Sweden). The ROV system consisted of several parts. The ROV itself was equipped with different additional sensors. All power supply and control units were placed in a Scott-Tent on the surface close to the access-hole. Communication between the surface units and the ROV was set up via a 200m long fiber-optics tether (umbilical). The tether contained copper wires for power supply and one fiber for all controls and data exchange. The tether was ordered to be of 300m length, but was delivered 100m too short for unknown reason, limiting the operation range to about 180m radius around the access-hole.

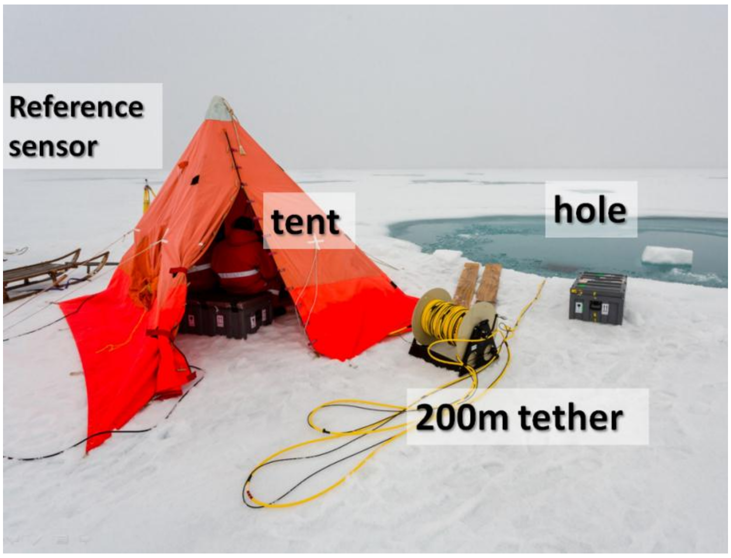

Figure 3: typical setup of a ROV launch site. The access-hole is located in the melt pond. Pilot and Co-pilot are controlling the ROV-survey from the orange Scott tent. The reference sensor recording incoming irradiance is situated on the yellow tripod behind the tent.

While access-holes could always be prepared through melt ponds during the 2011 IceArc expedition, this was not always possible this year. Still it was possible to make big enough holes by cutting with an ice-saw in up to 80cm thick ice in less than one hour. In one case the hole was made not close to the pond edge but far into the pond as ice-thickness was much smaller there.

ROV-SENSORS

The ROV was equipped with a variety of sensors shown in figure 4 which shall be described here:

ATTITUDE SENSORS & STANDARD ROV-COMPONENTS

The standard configuration of the *V8Sii ROV* is delivered with roll-, pitch-, heading- and a depth sensor. Due to the weak magnetic field the magnetic heading sensor started to spin easily resulting in uncontrollable ROV tumbling. This problem had been observed during the previous year as well. To avoid that problem it would be necessary to exclude the heading information from the stabilization software of the ROV. We managed to operate the ROV in the "VG horizon"-mode, where the heading information of a gyro-compass is used for stabilization. As this gyro-compass is strongly drifting, the pilot had to constantly correct for the caused self-rotation. The depth sensor was reset to zero while holding the ROV topside at the water surface in the access-hole before each survey.

CAMERAS

The main forward-looking camera was a *High Definition Compact Colour Zoom Camera OE14-502* (Kongsberg Maritime AS, Kongsberg, Norway) providing HD-resolution video and 10x zoom. Overlay information was added using a *HDO High Definition Digital Video Overlay & Video Scaler* Interface (OceanTools, Aberdeen, UK) for display in the pilot-tent on a HD-screen and for recording. It turned out that the camera provided much better pictures than the *Tritech Typhoon* (Tritech, Aberdeenshire, UK) used in the previous year. Unfortunately the angle of view proved to be too narrow for optical positioning using marker passing times. The time span between disappearance of the marker in the front camera and the actual passing was with six seconds - too long for positioning purposes. Fur future applications we therefore suggest to use a HD-zoom camera with wider view angle. View angle details for the Cameras used in 2011 and 2012 as well as for a suggested wider angle HD-zoom camera are given in the following table. Due to the changed aspect ratio even the wide-angled HD-camera does not reach the vertical view angle of the *Typhoon* camera used in 2011.

As in 2011 a *Tritech Osprey* (Tritech, Aberdeen, UK) was mounted as second camera on the ROV. Instead of using it as backward-camera, we mounted it upward looking parallel to the optical sensors. By that we were able to directly judge the properties of the ice above the sensors and in addition have good observation possibilities for algae-aggregates hanging from the sea-ice.

Camera-Type	Tritech Osprey	Tritech Typhoon	Kongsberg OE14-502	Kongsberg OE14-502-WA
used during	TransArc/IceArc	TransArc	IceArc	suggestion
resolution	SD	SD-zoom	HD-zoom	HD-zoom
aspect ratio	4:3	4:3	16:9	16:9
diagonal view angle	80°	66°	50°	70°
horizontal view angle	65°	52°	45°	63°
vertical view angle	**50°**	**39°**	**29°**	**38°**

The cameras were used both for documentation of the dives as well as photography of under-ice-fauna (when accidentally encountered) and under-ice measurement installations from other working groups. Images were extracted after each station onboard the ship using *VLC media player*.

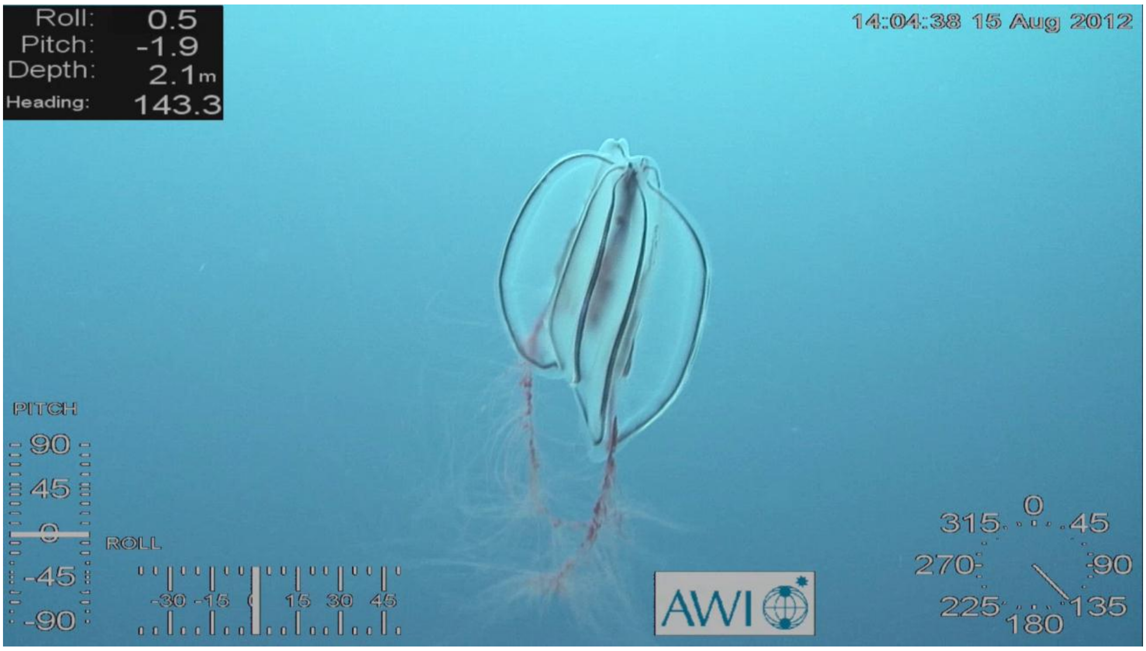

Figure 4: Image of a ctenophore, taken by the HD front camera of the ROV. The overlay shows time and date (upper right corner) as well as roll pitch depth and heading information.

SONAR & ALTIMETER

The same setup of Scanning Sonar *Micron DST MK2* (Tritech, Aberdeen, UK) and *DST Micron Echosounder* (Tritech, Aberdeen, UK) Altimeter was used as in the previous year. Initially the Altimeter was placed in the middle of the aft section of the ROV. During the first two stations we had the impression that altimeter data was of poorer quality compared to the last year. Influence by the metal arch over the altimeter was likely the cause, as repositioning the altimeter improved data quality. Sensor positions are shown in the figure to the right.

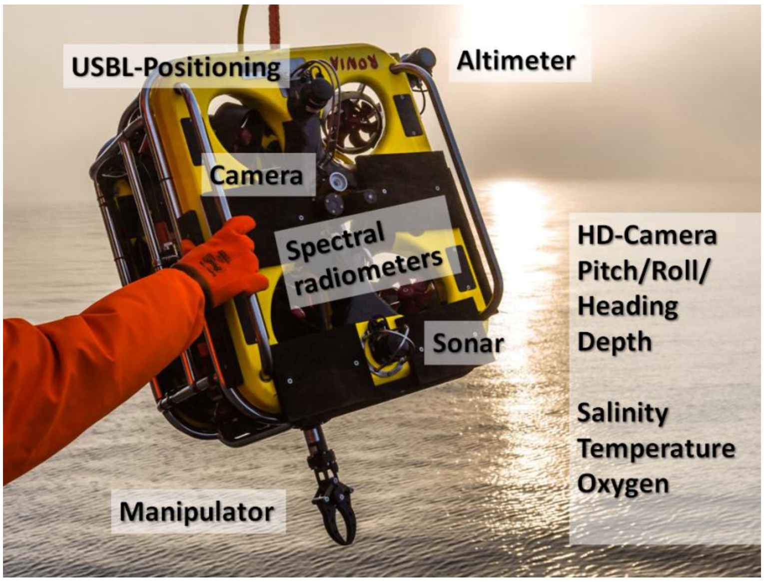

Figure 5: Positions of the various sensors on top of the ROV. Sensors mentioned in the right box are placed invisibly in the centre of the ROV-Body.

USBL-POSITIONING SYSTEM

The use of a *Tritech Micron Nav* (Tritech, Aberdeen, UK) USBL (Ultra-Short-Base-Line) positioning-system facilitated ROV surveys compared to the previous years. Before the cruise it was questionable how well the system would work in our conditions diving in very shallow depths directly under the highly reflective ice. Due to this untypical dive geometry Ocean modules suggested a setup where the transducer was installed upside-down (upward-looking) on a solid 9m long bar and the receiver unit on the bottom starboard aft corner of the ROV. This setup worked well, though it caused serious losses in positioning-quality in one angular segment due to reflections from the pole itself. Even with this method it was difficult to obtain a position behind bigger ridges. The mounting position of the ROV-transponder was delicate and on 16th August the transponder cabling got seriously damaged during transport. We were luckily able to repair the transponder but due to that incident we changed its mounting position to the earlier position of the altimeter in a well protected spot. Accordingly the dunking transducer was afterwards mounted in its normal position only about 1m below the ice-water interface. Surprisingly we did not encounter any loss of data quality. In case of strongly deformed ice the transducer was lowered further down up to 6m to reduce shadowing by ridges. In general we can conclude that USBL-positioning was providing a good positioning. The range of the position error is similar to the positioning by marker passing-times used during TransArc but increasing with the distance from the Transducer. Difficulties occurred in some stations to match the acquired USBL-positions with the positions of marker poles measured by handheld GPS at the surface. There seems to be some distortion between both systems, which could be influenced by strong under ice currents, as biggest distortions are found on days with rather strong under-ice currents. These effects need to be evaluated closer to increase future positioning accuracy.

OPTICAL SENSORS

As in the previous operation we used two *RAMSES-VIS* spectral radiometers (TriOs, Rastede, Germany) onboard the ROV. The irradiance sensor (RAMES-ACC) with cosine collector and the radiance sensor (RAMSES-ARC) were both equipped with an IP-module measuring inclination and pressure. They were mounted next to each other together with the upward looking camera in a central hole of the ROV, providing better mechanical protection and improved measurement geometry compared to the year before. Both sensors were powered by the ROV and exchanged data via the fiber link in the tether. A surface reference sensor was placed on a tripod close to the pilot-tent. For future applications we suggest the use of a sensor measuring water extinction directly, to overcome the drawbacks of the current method of extracting extinction-coefficients from depth profiles. A TriOs *VIPER-VIS* (TriOs GmbH, Rastede, Germany) could be easily integrated in the data acquisition system and can be fixed directly to the ROV.

CTD & O_2 SENSORS

In cooperation of the biogeochemistry group onboard (especially Frank Wenzhöfer & Jörn Patrick Meyer from MPI Bremen) further sensors were mounted on the ROV. They used an external data-logger and just received power-supply from the ROV. To be able to obtain CTD profiles and measurements along transects a temperature and salinity sensor was integrated together with an oxygen sensor. Data was downloaded after each station and will after calibration be included into the dataset of optical data.

SURFACE UNIT & RECORDING

The surface unit consisted of a huge rack including the power converter, ROV-surface-box, USBL-surface-box, OceanTools HDO Overlay Interface and a computer for recording. The video signals of both cameras were synchronously displayed on two screens in front of the pilot using the pilot-control-unit to steer the ROV. All three optical sensors were connected to a Laptop using a 4 channel IPS box (TriOs, Rastede, Germany) where data was recorded using the manufacturers sensor control software MSDA_XE. Sampling intervals were chosen according to light conditions between 2 and 10 seconds.

Position & Sonar data were displayed on one screen using *Seanet pro* (Tritech, Aberdeen, UK). All data streams were gathered and synchronously recorded on the computer using the software Spot.On (Ocean Modules, Åtvidaberg, Sweden) operated by the co-pilot. Unfortunately we discovered that the system clocks of all four involved systems (computer, rov, overlay, laptop) were running asynchronously even after synchronization with the Polarstern time-server. To compensate for that deviation we resynchronized the clocks regularly and noted all time-offsets with an accuracy of ±1 second. Additionally we discovered, that Spot.On is not actually recording all streams synchronously but with a lag of several seconds between each other, making data analysis very difficult. To estimate Spot.On recording and playback lags we performed synchronization experiments in the lab to be able to correct for these offsets. This timing problem is seriously reducing the quality of recorded data and needs to be addressed for future applications!

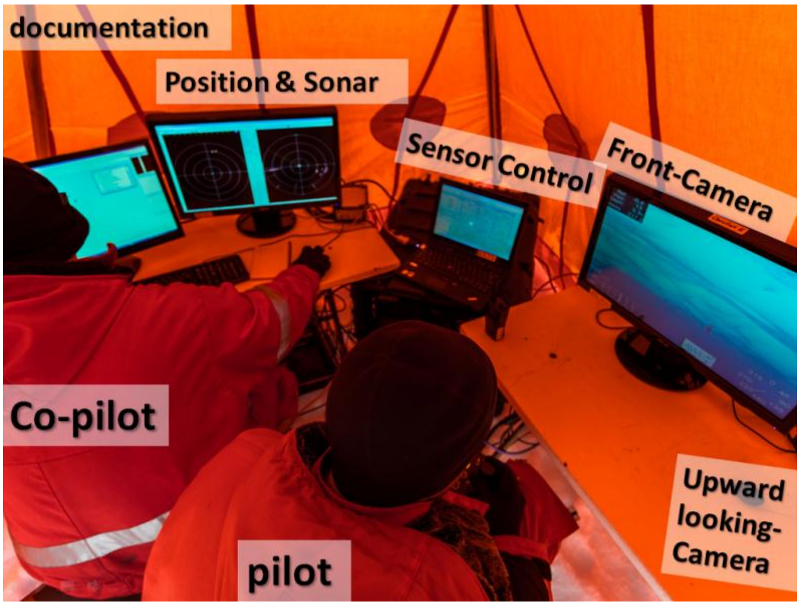

Figure 6: Control and documentation screens in the pilot tent.

Due to the short length of the USBL-transducer-cable, it had to be installed through a 12cm core-hole directly next to the pilot tent decreasing flexibility of transducer positioning. Limited space due to increased amounts of electronics inside the tent compared to the previous year made it impossible to place the gas heating inside the tent.

POWER SUPPLY

As we experienced major problems with the power supply during 2011, new equipment was used during IceArc. This time we used two *Honda EU 30i* (Honda Deutschland GmbH, Offenbach, Germany) power generators coupled together by the manufacturers coupling cable. Due to the inverter technology this setup supplied very stable 6kW. Both generators had to be run in continuous-“bunny”-mode during ROV-operations, as the eco-“turtle”-mode was in some situations not quick enough to supply enough power. The fuel tanks were enough for about 6-8 hours of operation and had to be refilled once per ice-station.

STANDARD OPERATION PROCEDURE

Due to the deployment of benthic lander equipment, station times were regularly around 3 days, leaving enough time for ROV operations.

The first step was the selection of the floe by helicopter search. Floe properties had to match the requirements from several working groups and lie in vicinity of the lander deployment site. The selected floe was marked using red flags and a Novatech RF-700A1 (MetOcean, Dartmouth, Canada) VHF Radio Beacon to ease relocation with the vessel. When reaching the floe, the gangway was deployed onto the ice. A polar bear watch from the bridge was organized during daily working hours from 9.00-20.00. During night hours as well as during bad visibility each working group on the ice was responsible for their own for polar bear safety.

On the first day/afternoon, we usually prepared the access-hole and marked the profile-lines. Ice thickness, snow thickness, freeboard and scattering layer were measured each 10m at the marker positions along the profiles. In some cases with little risk of polar bear encounters, we already set up the tent close to the access-hole.

Depending on light conditions, work continued on the (early) morning of the second day. While all electronics of the ROV was set up in the tent, the marker sticks were placed under the ice along the marked profiles ROV setup took around one to two hours, before surveys could be started. To reduce temperature related problems, the ROV itself was only taken out on the floe shortly before launch. All surveys were timed in a way that measurements were taken during the time few hours before and after solar noon.

After a first orientation dive, we conducted several dives along the transects in the constant depth mode. Dive depth was mostly 1.5-2m. Pitch and roll values were kept below 10° by the pilot. Start and end of profile measurements as well as passing markers and any other events were marked in the Spot.On-Software by the co-pilot. When measurements along the profiles were completed, single point measurements next to chosen marker positions were taken directly at the ice-water-interface. Bio-optical cores were afterwards taken in these locations and spectral albedo measured at all marker positions. Further optical data was gathered while diving grids between and around the marked profiles and measuring depth profiles to determine sea-water extinction. Additional optical experiments were conducted in some stations.

Depending on the station plan, ROV operations were either continued on the same site during the next day, or moved to a second site. In areas with little risk of a polarbear encounter we left the equipment packed in the tent on the ice. This is not recommended for future operations, as we encountered several problems restarting the cold equipment in the morning.

The complex ROV setup proved to be manageable on the floe during ice stations of a minimum length of 10 hours. For further ease of operation especially during colder seasons, it could be helpful to mount all electronics permanently in a lightweight isolated and heatable cabin mounted on a sledge. This sledge could be put on the ice by a crane and maneuvered to the site using skidoos. Such technique can strongly decrease the need of station time as about 2-4 hours could be saved during setup and packing.

After or during survey we tried to shoot aerial images, with the imaging system installed on the EM-Bird. In many of the stations this was not possible due to bad flight weather. Furthermore it proved to be difficult to actually take pictures of the right part of the floe. For future work we suggest to use a kite or balloon carrying a little camera, to obtain aerial pictures. This will allow for aerial pictures even during worse flight conditions, when the high resolution system onboard the EM-Bird is not available.

TECHNICAL PROBLEMS

Even though the ROV system was operating mostly well, we had several technical problems, which shall be documented in the following:

- One of the biggest problems was a temperature sensitivity of the FVCT (Fiber Vehicle Control Tube). Due to this error the ROV showed the "NO LINK"-Error on startup. While the problem disappeared after the 5th try on the first stations, it was not possible to power up the ROV on later stations. Troubleshooting in the lab revealed, that the ROV was not starting when the Temperature of the front region of the FVCT was under a certain threshold. This problem was overcome by heating the FVCT with a hot air pistol before start up. Depending on air temperature this took up to 20 minutes.

Figure 7: The damage of the MCT, likely caused by a leak in the tube.

- The MCT got damaged probably by leaking water and two thrusters had to be exchanged due to an internal short-circuit.
- One Thruster lost its propeller during operation
- We had a major defect in the FVCT. Exchanging all circuit boards did not help as exactly the HD-graphics card for which we had no spare part was damaged. Our technician succeeded with the assistance of the manufacturer via email, to repair the circuit-board.
- Spot.On lead to some software problems. The USBL-position stream stopped working after a while even though the *Micron Nav* was still acquiring a position. The survey needed to be restarted and all marked positions on the map, as well as all streams had to be reentered.
- During transport of the ROV, the connector of the USBL-Transponder got ripped out of the casing. Luckily we were able to reorganize the Tritech acoustic equipment and use the second aux-connector enabling further use of the USBL-system, after sealing the opening with special resin.
- During the last two stations, the SD video-overlay did not show up.
- One morning we had problems starting the generator, because the spark plugs were full of soot. Cleaning of the spark plugs, rewarming inside the ship and ventilation solved the problem.
- Several times, the incoming sensor had to be reconnected, due to some data transfer problem.

ROV-STATIONS

In this section we are describing the characteristics of each ROV-station, L-Arm measurements and helicopter stations are listed further down. Ice station overview maps and plots of meteorological parameters are available at http://epic.awi.de/31661. The following table gives an overview about all ROV-Dives on all different stations.

Station	Date	Number	Spot-On Time	Comment
224	10. Aug 12	#1	11:26-12:49	
		#2	12:54-14:02	
		#3	14:06-14:38	
		#4	16:29-17:19	
		#5	17:25-18:20	
237	15. Aug 12	#1	7:15-7:35	bad navigation, coordinates changed after dive
		#2	7:39-10:19	
		#3	10:22-11:21	biocores, grid 1
		#4	11:35-12:18	grid 2
		#5	12:20-13:08	to Oze/Eddy
	16. Aug 12	#1	7:29-8:29	
		#2	8:31-9:14	
		#3	9:17-10:40	
		#5	14:47-14:51	no data
		#bio	no record	rov defect
		#bio2	no record	rov defect
255	20. Aug 12	#1	4:19-4:48	tests, one bad profile/positioning
		#2	no record	nothing
		#3	7:46-8:42	Profiles
		#4	8:57-9:29	depth profile and bad positioning
323	05. Sep 12	#1	2:39-3:20	Profile
		#2	-	no data
		#3	3:24-4:16	profile & depth profile
		#4	4:18-5:00	grid (Bundesadler)
		#5	5:02-7:19	Eddy 1 (Foto)
		#6	7:22-8:21	Eddy 2 & 4m grid (Video missing)
335	08. Sep 12	#1	23:51-0:39	profile flat
		#2	0:41-1:27	profile ridge & Larysa
		#3	1:30-2:14	depth profile
		#4	2:16-2:37	- rov failure
		#5	4:14-4:53	grid
		#6	4:56-5:04	pitch & roll
		#7	11:55-12:57	bio-suck
		#8	13:45-14:12	Fotoflight (Profiler)
	09. Sep 12	#1	2:29-3:07	search dive & Pferdegrid
		#2	-	empty
		#3	3:38-4:14	grid Marcel
349	19. Sep	#1	5:00-6:36	Orientation (Cap on Incom)
		#2	06:58-8:23	Susi + poth profiles + ponds
		#3	8:25-9:13	depth @ M21 10m profile
		#4	10:43-11:47	susi 2
360	22. Sep	#1	8:58-9:41	Profile y & 10 degree pitch
		#2	9:43-10:55	pitch 20 & profile x
		#3	10:59-12:07	depth & base profile snow removal
		#4	12:09-12:44	snow removal experiment
	23. Sep	#1	8:47-10:07	Profile y & Profiler
		#2	10:13-11:11	Profile x & IMB, Coring, Sedimenttrap
384	29. Sep	#1	08:39-9:39	Images of Station & x profile
		#2	9:42-10:48	Profile y & Grid under Station & Sensor search

ICE-1

Date:	9.8.2012- 11.8.2012	**Station#:**	PS80/224
Position (USBL):	84.0° N 30.0° E		

Air-temperature: -3 to 0 °C **Wind-speed:** 0 to 5 m/s **Drift speed:** 0.1 to 0.3 kn

Weather: mostly overcast, some clear sky during ROV survey

Global radiation: 50 to 400 W/m²

Ice type: FYI, heavily deformed ridge and two different level ice thicknesses

Melt ponds: dark and light blue melt ponds, first frazil ice-cover forming

Surface: 5 cm or 10cm degraded surface layer on thin and thick level ice, respectively.

Measurements: two profile lines(100m, 117m), bio and eddy images, depth profile at M9, BioCores, photo-pitch-flight, field survey, photos and measurements at radiation station.

(Aerial-)Image:

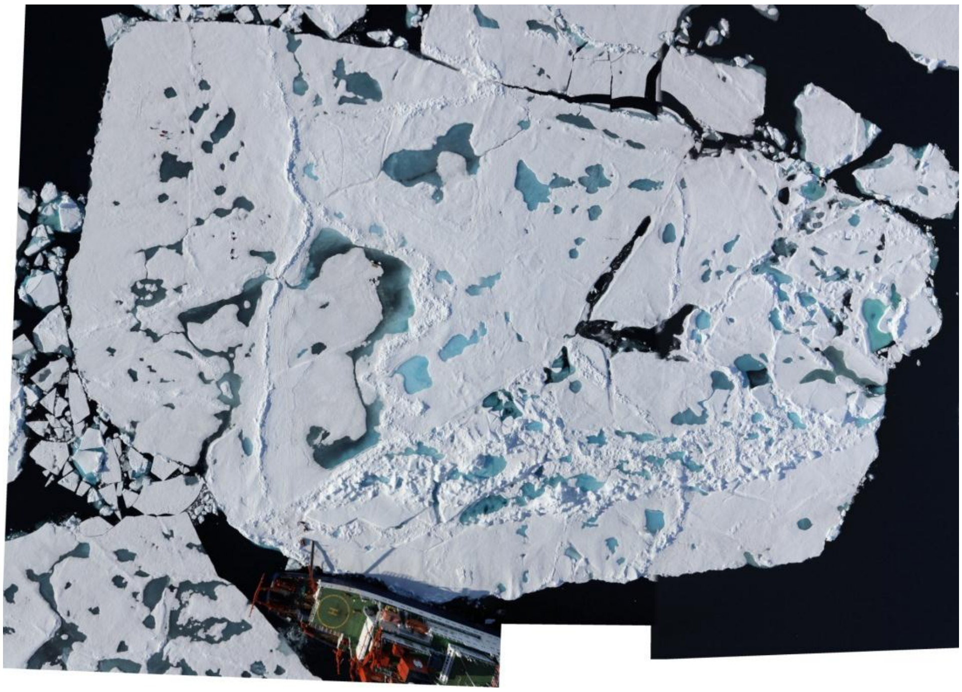

Coordinate plot:

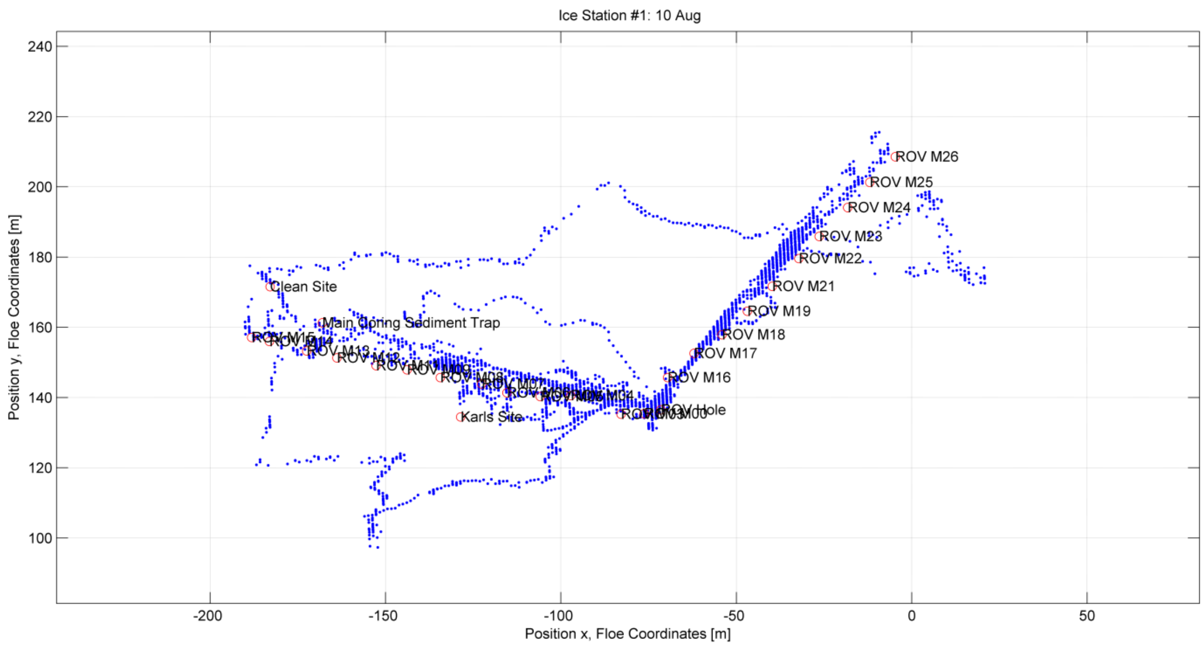

ICE-2

Date: 15.8.2012- 17.8.2012 **Station#:** PS80/237

Position (USBL): 83.9477° N 76.8603° E

Air-temperature: -3 to 0 °C **Wind-speed:** 5 to 12 m/s **Drift speed:** 0.2 to 0.6 kn

Weather: overcast

Global radiation: 50 to 250 W/m²

Ice type: very rotten FYI (15.8.), thicker MYI with light blue pond (16.8.)

Melt ponds: dark and light blue melt ponds, thin ice cover (1-3 cm)

Surface: ~15cm very degraded surface layer on very rotten ice (wet feet day)

Measurements: two profile lines(2x100m), bio and eddy images, depth profile at M5, BioCores, profile at 4m and 10m, field survey, measurements of light and dark blue pond, draining pond

(Aerial-)Image: profile y and aerial image of second day (inlay)

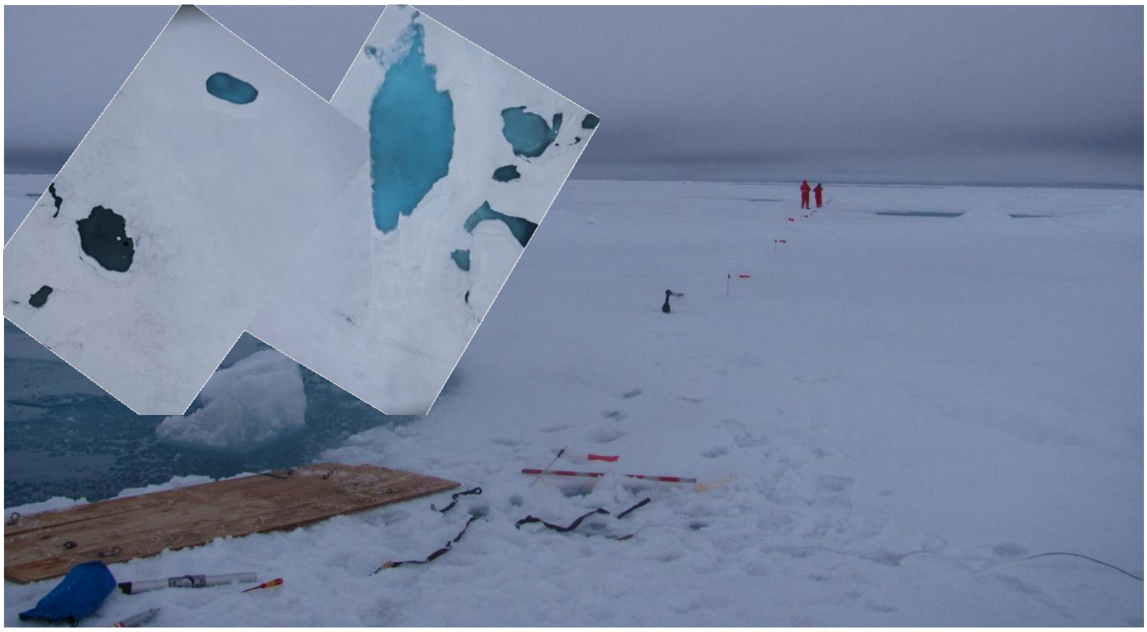

Coordinate plot:

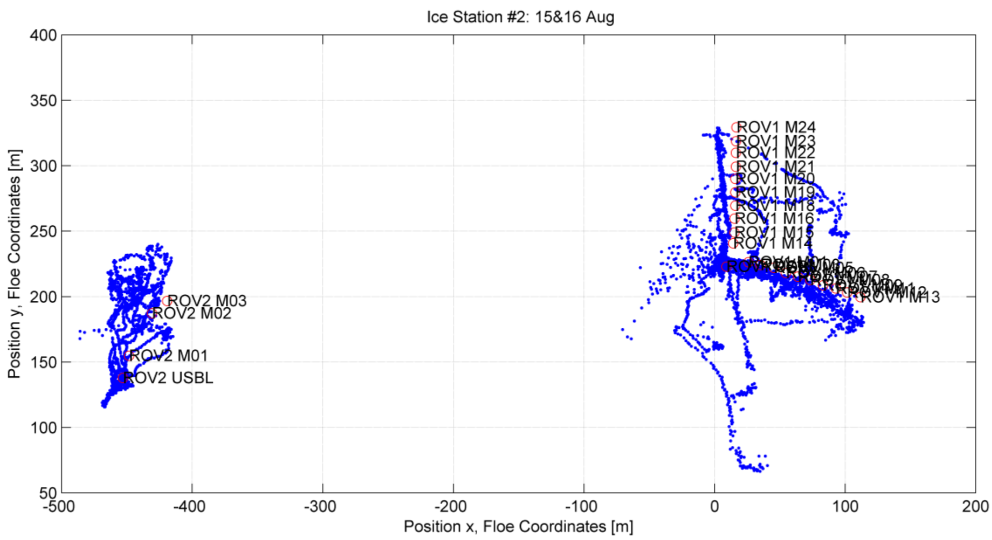

ICE-3

Date:	20.8.2012- 22.8.2012		**Station#:**	PS80/255	
Position (USBL):	82.8649° N	109.861733° E			
Air-temperature:	mostly 0°C	**Wind-speed:**	7 to 15 m/s	**Drift speed:**	0.2 to 1 kn
Weather:	overcast				
Global radiation:	10 to 200 W/m²				
Ice type:	FYI				
Melt ponds:	thin ice cover (5-7 cm)				
Surface:	5cm very degraded surface layer on very rotten ice				

Measurements: two profile lines(2x100m), compass problems (H=1600nT), ROV-failure on second day. bio and eddy images, depth profile

(Aerial-)Image: profiles

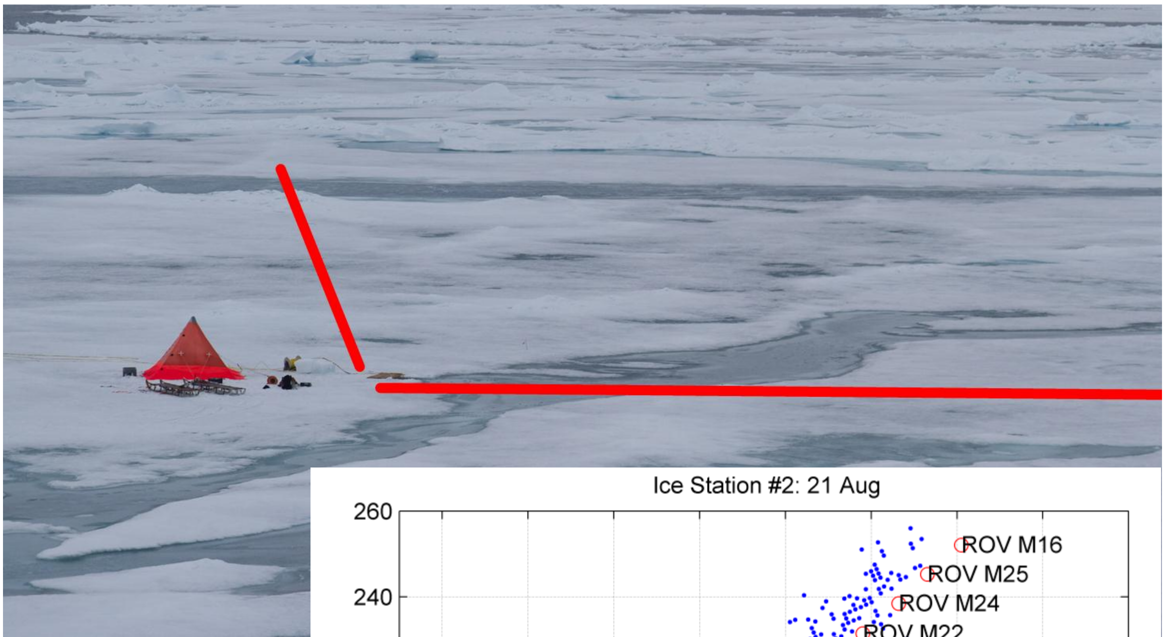

Coordinate plot:

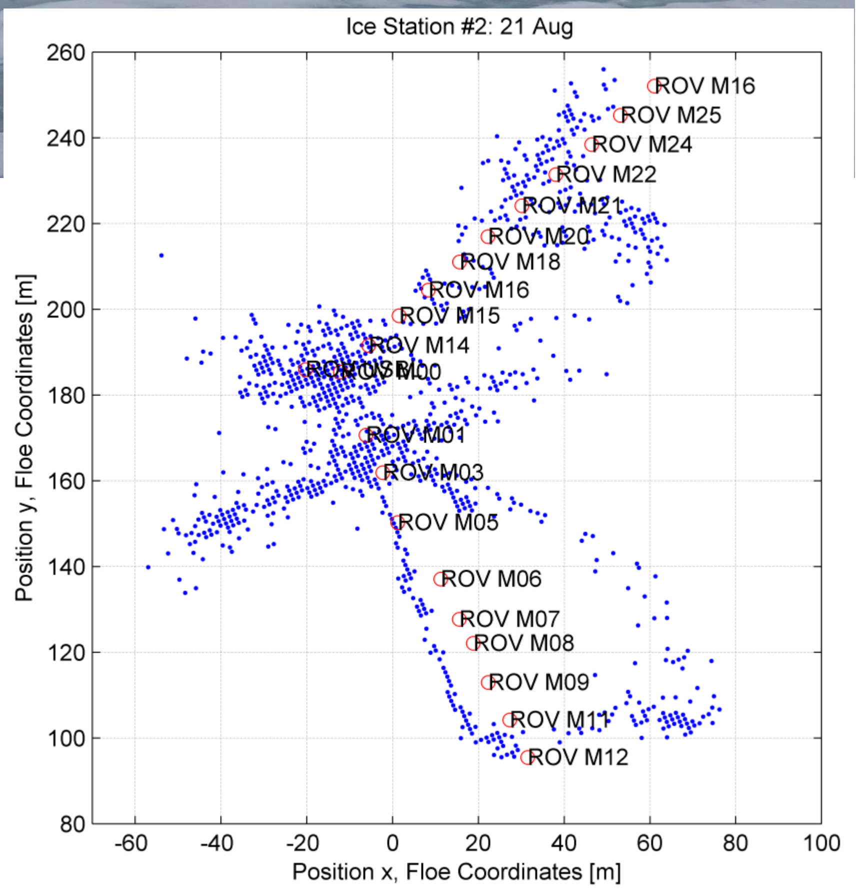

ICE-4

Date: 25.8.2012- 26.8.2012 **Station#:** PS80/277

Position (USBL): 82.8805° N 129.8673° E

Air-temperature: mostly 0°C **Wind-speed:** 0 to 5 m/s **Drift speed:** 0.1 to 0.4 kn

Weather: overcast

Global radiation: 10 to 160 W/m²

Ice type: FYI & MYI

Melt ponds: ice covered

Surface: 5cm very degraded surface layer

Measurements: only L-Arm measurements, deployment of seasonal IMB

(Aerial-)Image: seasonal IMB

Coordinate plot:

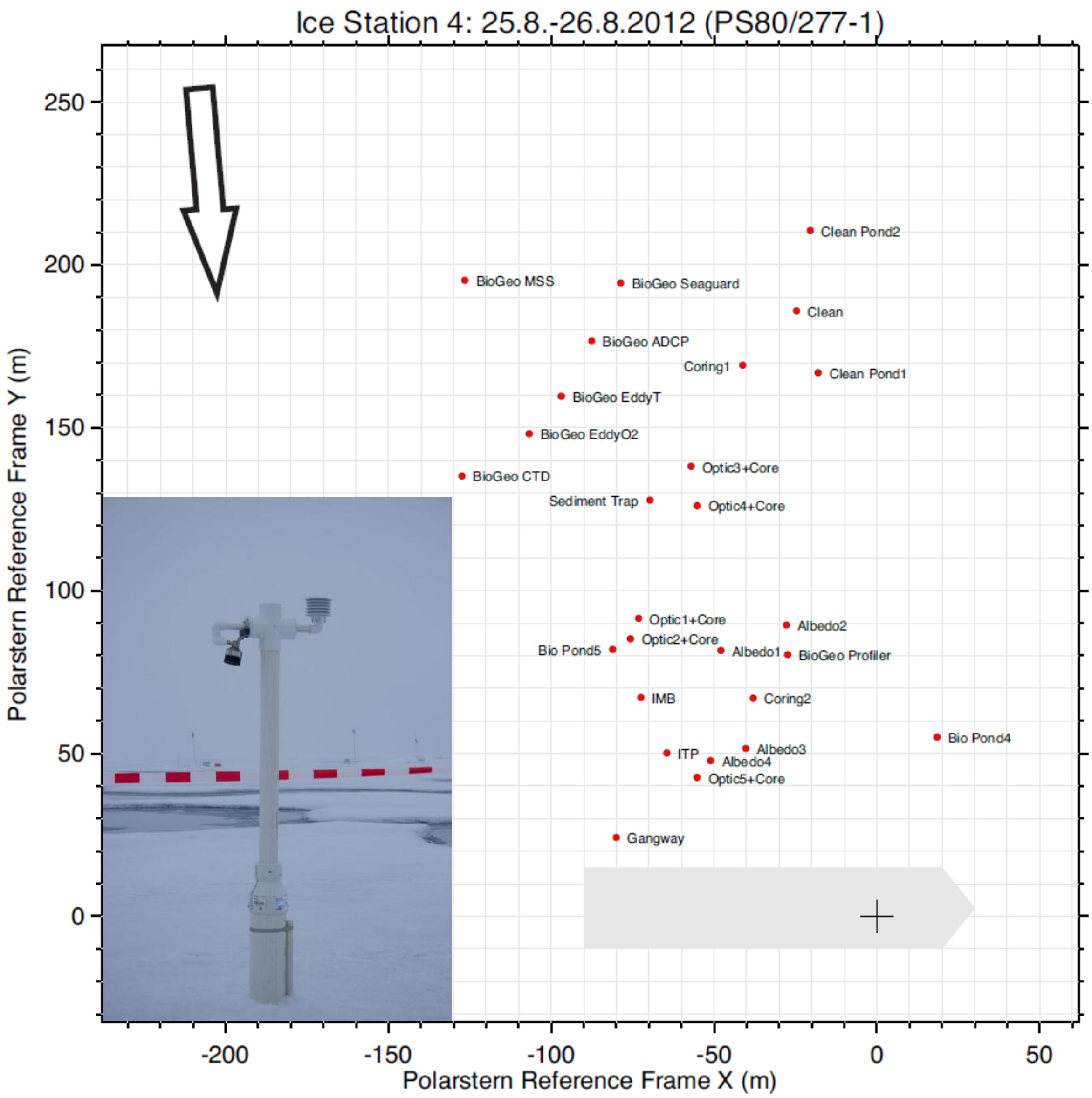

ICE-5

Date: 4.9.2012- 5.9.2012 **Station#:** PS80/323

Position (USBL): 82.8828° N 130.7587° E

Air-temperature: mostly -3°C **Wind-speed:** 2 to 7 m/s **Drift speed:** 0.0 to 0.5 kn

Weather: overcast

Global radiation: 10 to 300 W/m²

Ice type: FYI

Melt ponds: ice covered and partly snow covered

Surface: 4cm surface layer under 0-6cm of snow

Measurements: two profiles(105m & 100m), depth profile at M5, photos of biogeo equipment

(Aerial-)Image: ROV hole indicated by arrow

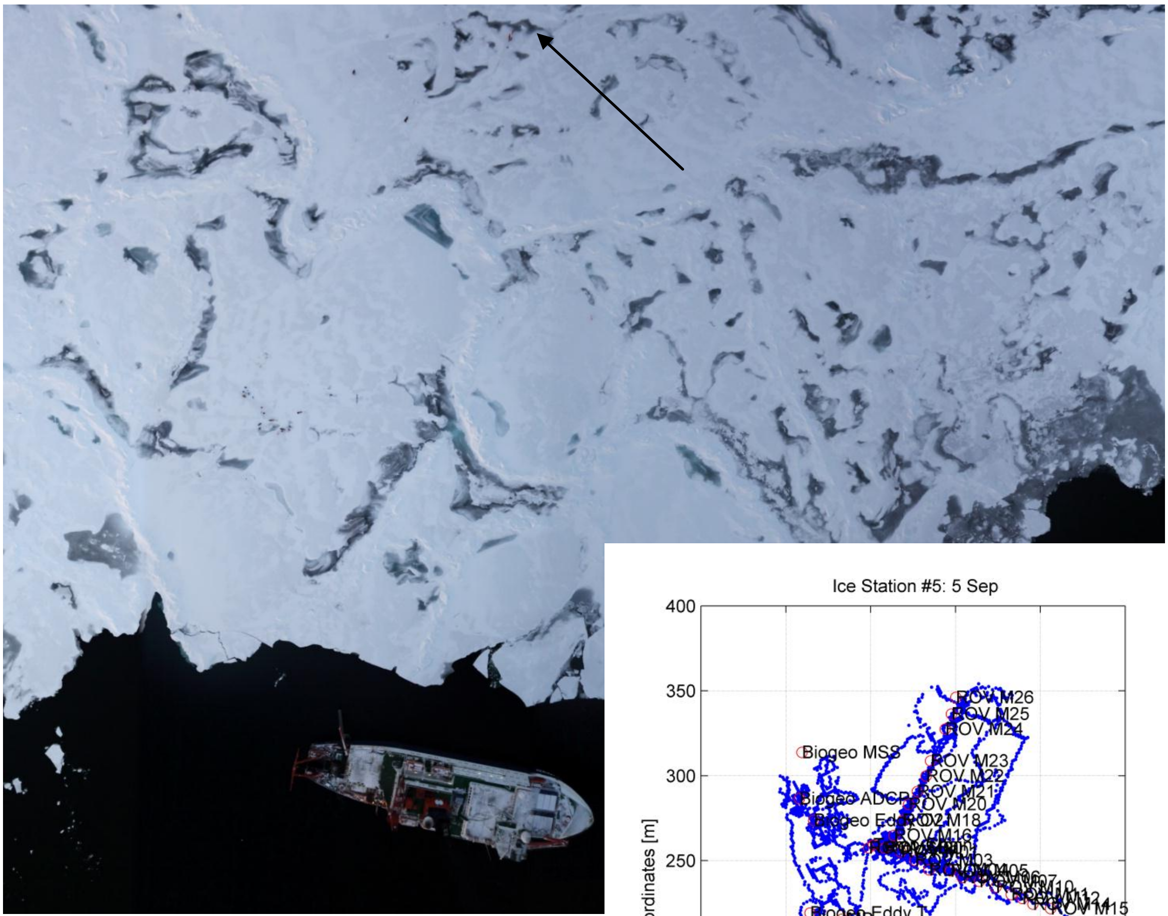

Coordinate plot:

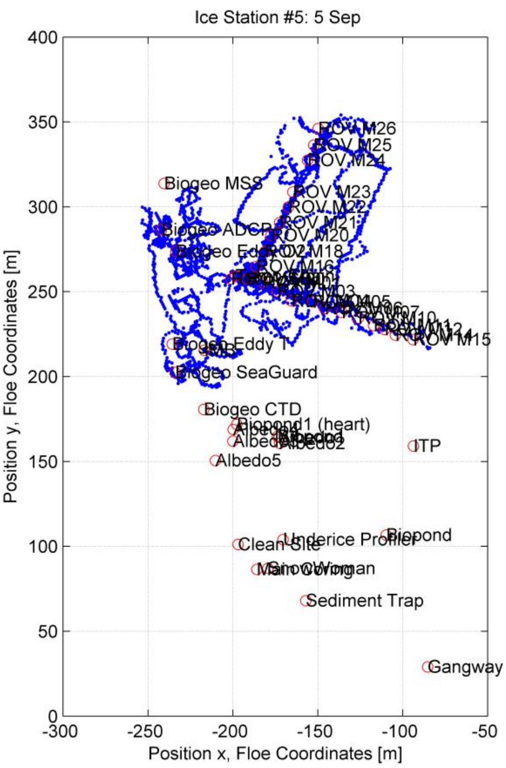

ICE-6

Date: 7.9.2012- 9.9.2012 **Station#:** PS80/335

Position (USBL): 85.0566° N 122.5233° E

Air-temperature: -3 to 0 °C **Wind-speed:** increasing from 0 to 12 m/s

Drift speed: 0.0 to 0.5 kn on 8.9. and 0.5 to 0.9 kn on 9.9.

Weather: mostly overcast

Global radiation: 0 to 100 W/m²

Ice type: FYI and some new ice

Melt ponds: ice covered and partly snow covered

Surface: 10cm surface layer under 0-12cm of snow

Measurements: 8.9.: two profiles(80m & 100m), depth profile, roll-experiment, photos of biogeo equipment, field survey
9.9.: field survey

(Aerial-)Image:

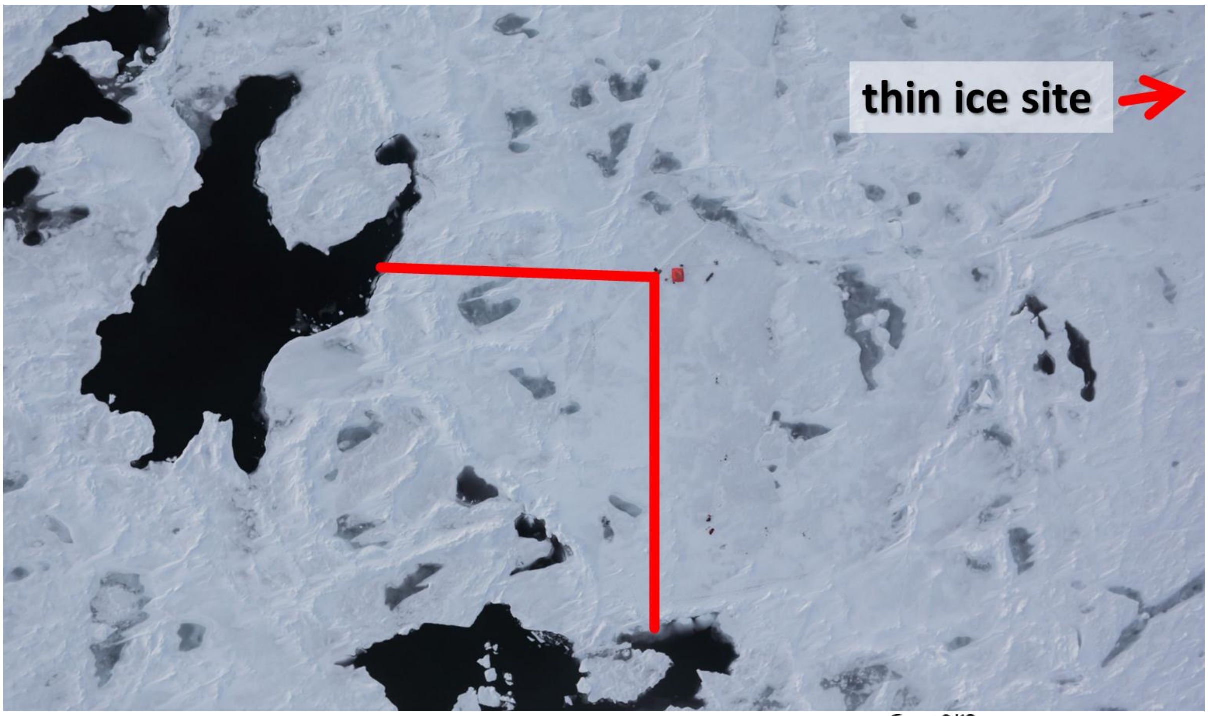

Coordinate plot:

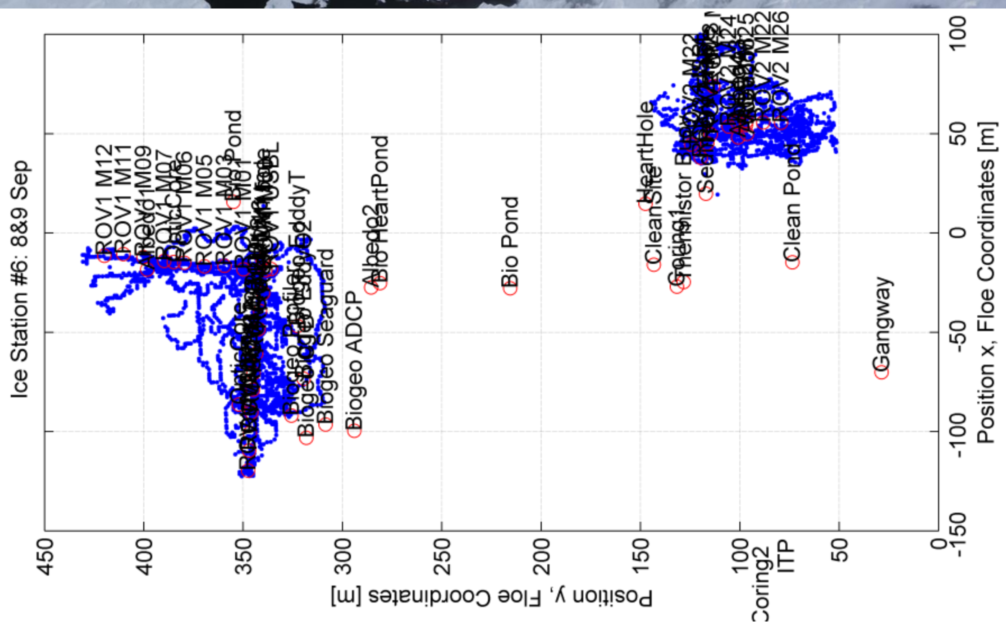

ICE-7

Date:	18.9.2012- 19.9.2012		**Station#:**	PS80/349	
Position (USBL):	87.9253° N	60.9516° E			

Air-temperature: mostly -4 °C **Wind-speed:** around 2 m/s **Drift speed:** 0.0 to 0.1 kn
Weather: overcast
Global radiation: 0 to 10 W/m²
Ice type: thick FYI, strongly deformed on the bottom →could be MYI
Melt ponds: ice covered and partly snow covered
Surface: 10cm surface layer under 0-2cm of snow

Measurements: two profiles (80m & 100m), depth profile at M21, algae video & sampling, pitch dives, profile at 10m depth, under ice mosaic video, bio measurements & visit of coring site

(Aerial-)Image:

Coordinate plot:

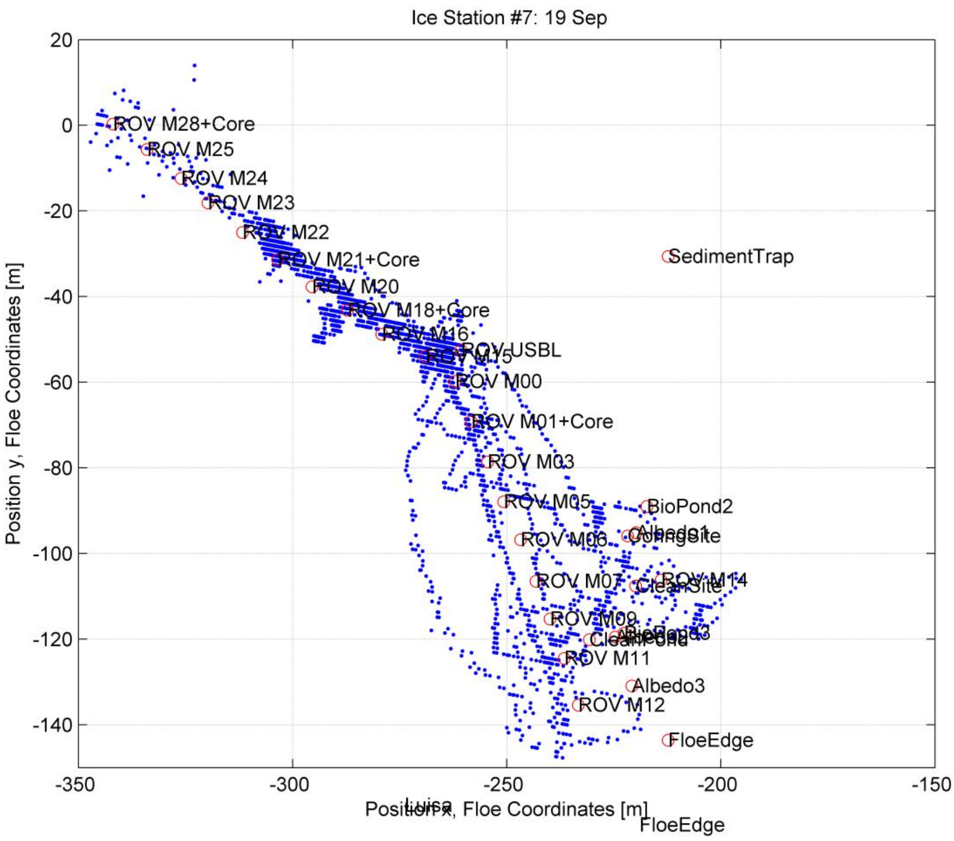

ICE-8

Date:	21.9.2012- 23.9.2012	**Station#:**	PS80/360
Position (USBL):	88.8256° N 58.5325° E		

Air-temperature: -12 to -6 °C **Wind-speed:** 5 to 10 m/s **Drift speed:** 0.2 kn
Weather: overcast
Global radiation: < 10 W/m²
Ice type: FYI/MYI
Melt ponds: snow covered and frozen through
Surface: 0-17cm surface layer under 1-6cm of snow

Measurements: two profiles (2x 100m), depth profile at M5, pitch dives, tent shadowing, snow removal experiment, device images & visit of coring site

(Aerial-)Image: profile x

Coordinate plot:

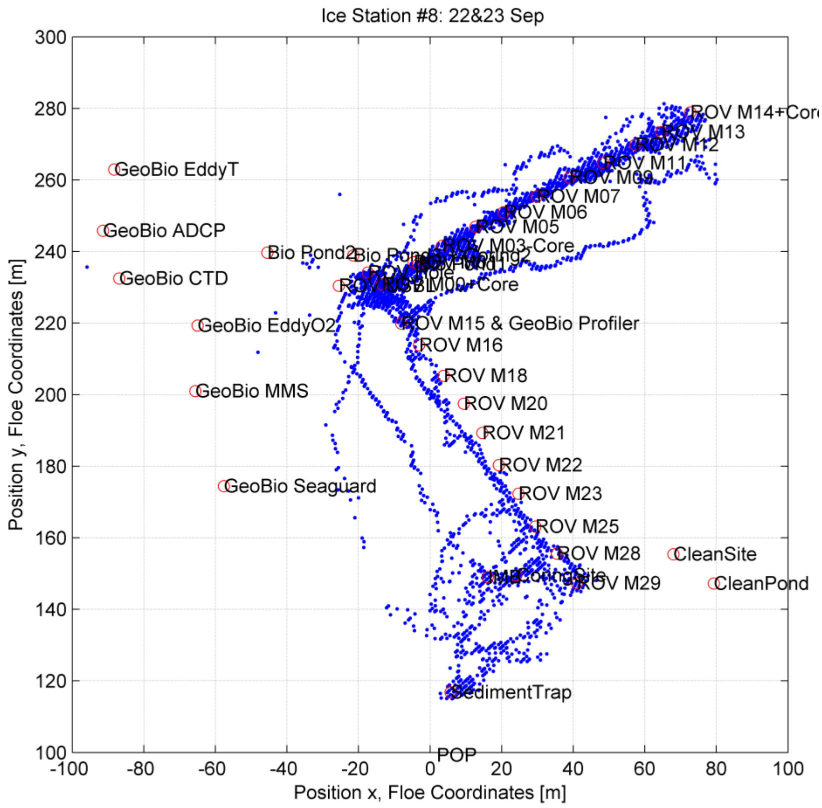

ICE-9

Date: 28.9.2012- 29.9.2012 **Station#:** PS80/384

Position (USBL): 84.35° N 17.73° E

Air-temperature: -9 °C **Wind-speed:** 5 m/s **Drift speed:** 0 to 0.2 kn

Weather: overcast

Global radiation: < 10 W/m²

Ice type: FYI/MYI, new ice repeated visit

Melt ponds: snow covered and frozen through

Surface: 2-12cm surface layer under 1-10cm of snow

Measurements: two profiles (60 &100m), depth profile at M5 (FYI) & M15 (new ice), device images, field survey, smiley in new ice

(Aerial-)Image: see long-term-station or ICE-1

Coordinate plot:

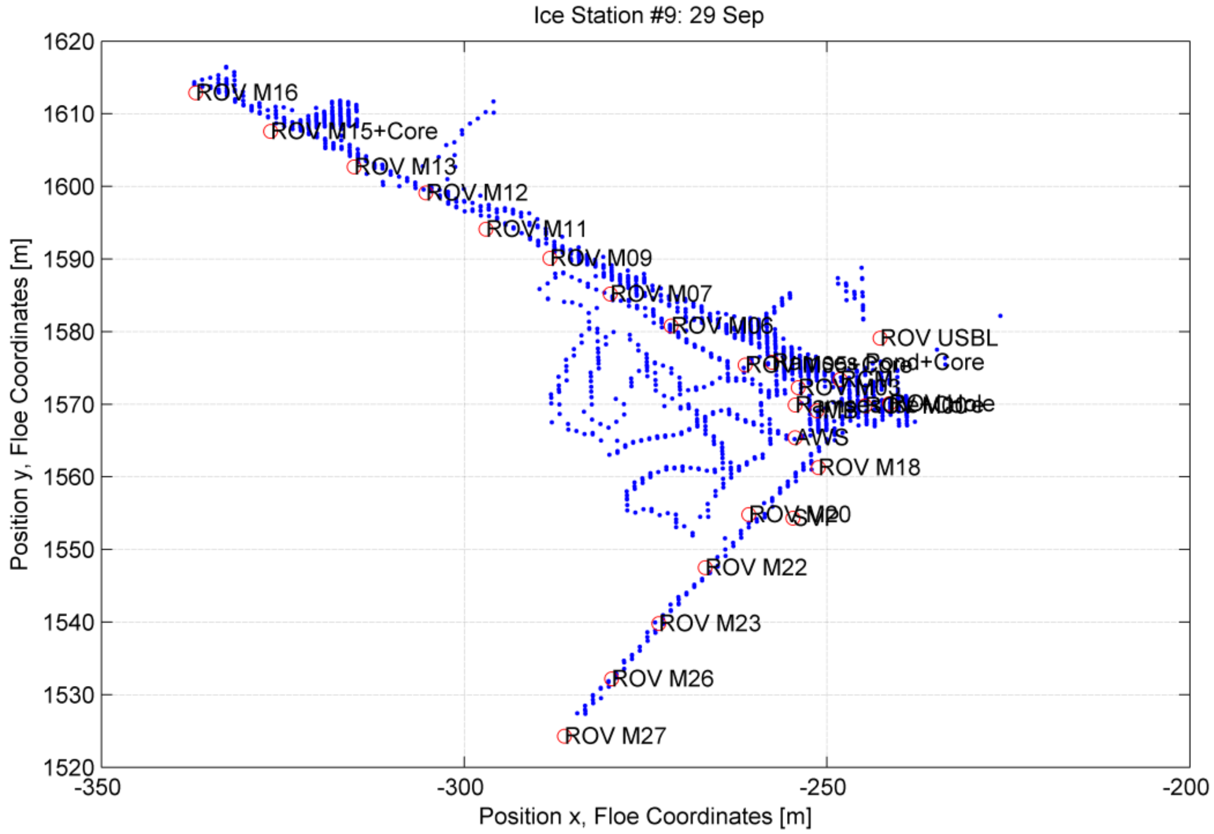

OPTICAL MEASUREMENTS

Here we present some preliminary data examples from the first icestation. In the unprocessed transmittance histogram we can clearly distinguish three modes. One is originating from the bare ice transmission of approximately 1-4%. The ponds form a wide mode between 15% and 25% while values around 60% can be associated to ice edge data. Spatial distribution of transmittances is shown together with an aerial-picture. The long term station was located in the area of rather low light transmittance with thicker ice indicated by the lighter pond color.

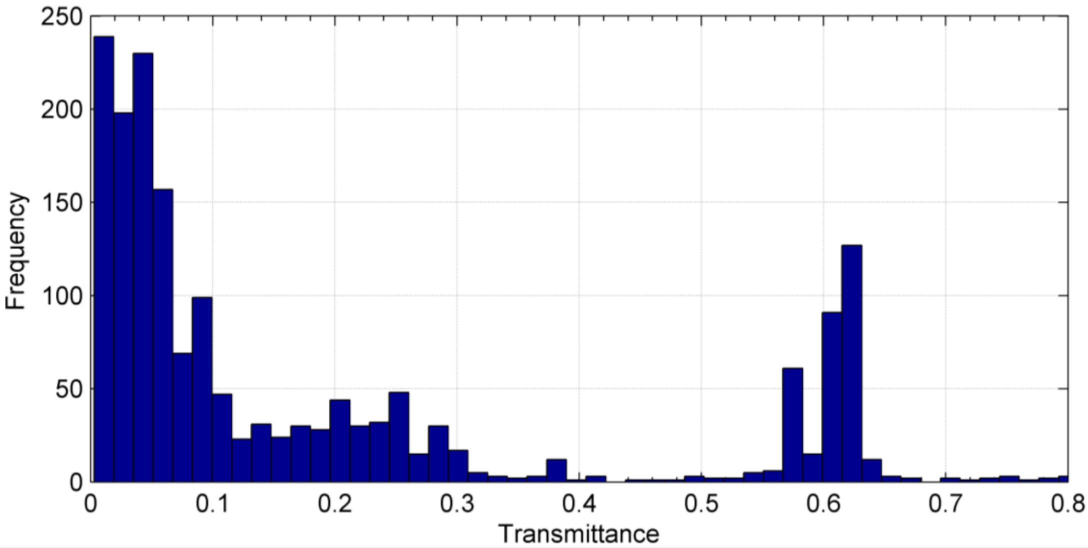

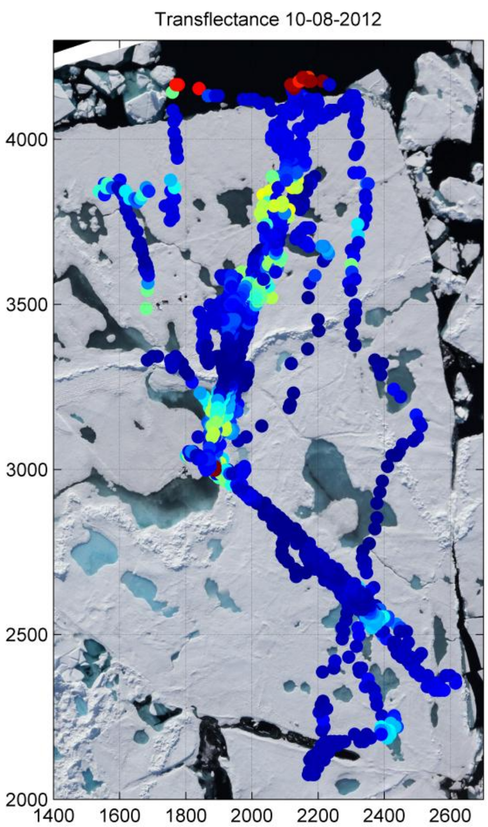

Figure 8 (top): Frequency distribution of light transmittance on the first icestation. The three modes can be assigned to bare- and ponded ice as well as measurements at the floe edge.

Figure 9 (left): Spatial distribution of measured transflectance plotted on top of an aerial picture

Figure 10 (bottom): Draft (ice thickness) distribution as obtained from the ROV-altimeter data. Several modes are visible, with level ice <1m at the edges of the floe, level ice >1m around the radiation station and thicker ridged ice.

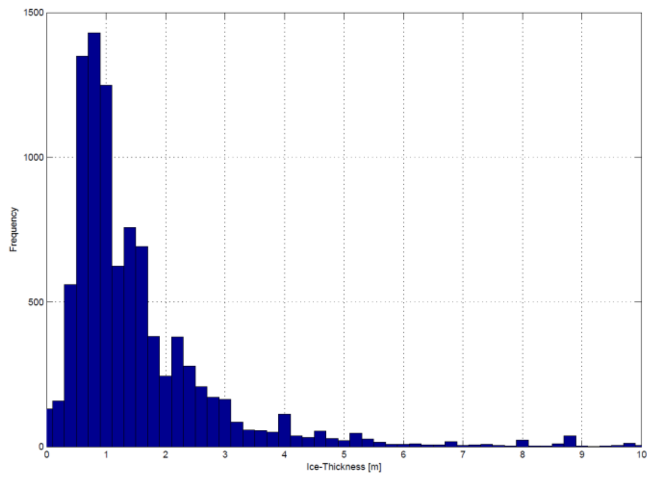

ALGAE-QUANTIFICATION

During the cruise we realized, that images from the upward looking camera could be used for quantification of under-ice algal-aggregates. As those aggregates mostly accumulate in any concave structure at the ice-water-interface, it is difficult to quantify their spatial distribution with the forward looking camera used in the year before.

Images were extracted all ten seconds from the dive videos and imported to MATLAB. Image edges were cropped to remove overlay and decrease the influence of exposure differences. Algae detection was conducted with the green channel of the RGB data. All pixels exceeding a value of 100 (maximum 255) were considered as algal aggregates. As this detection is not unambiguous, all images were displayed aside with the detections and checked for correct detection manually. Wrong detections were discarded for analysis. Pixels detected as aggregates were counted to compute areal coverage. Aggregate numbers were counted using the *bwconncomp()* function, providing also the amount of pixels within each aggregate. Aggregates touching each other within the resolution limits of the camera are therefore counted as one big aggregate. The camera was calibrated to convert from pixels to real area with the additional information given by the attitude sensors and the altimeter. At a distance of 80 cm from the ice, the length of one pixel corresponds to 3,1 mm.

The retrieved data was plotted using the USBL positioning data and size distributions were calculated assuming ideal circular shape to assess the impact of the miscounting of close-lying aggregates. Due to time offsets in the attitude data, only the spatial coverage was included in further analysis until now (Boetius 2012, under review).

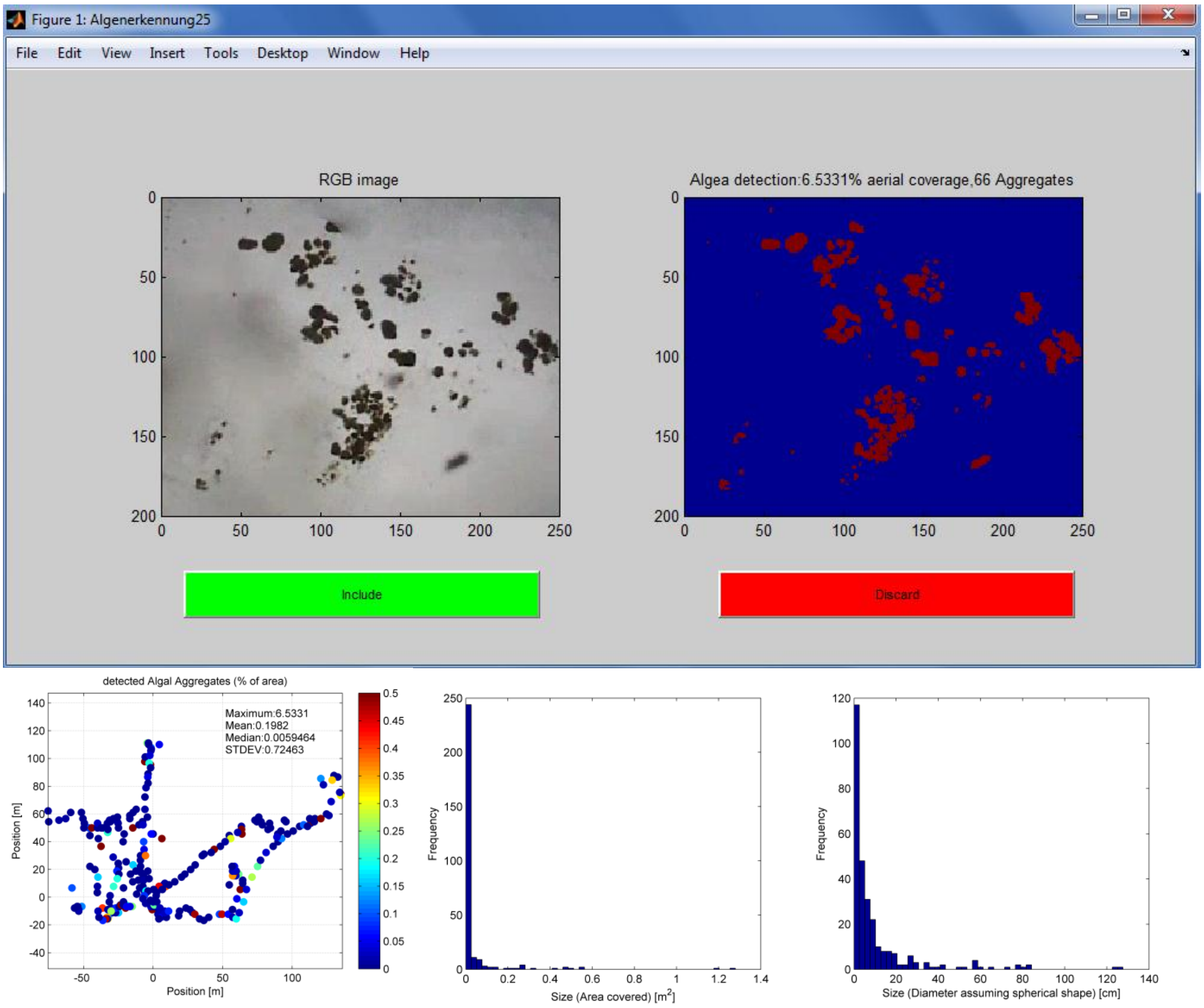

Figure 11: Upper image: Example of the software used to assess the quality of algae detection showing the RGB image to the left and the detection (algae marked in red) including the values for areal coverage and aggregate number on the right along with decision buttons in the bottom. Lower row: Spatial distribution of detected areal coverage (left), histogram of the true area covered by single aggregates (middle) and histogram of the calculated diameter assuming circular shape (right).

L-ARM OPTICAL MEASUREMENTS DURING ICEARC

Measurements of transmitted Light under the ice using an L-Arm as sensor carrier were recorded during Ice Station #4 on 26 August and on two Helicopter Ice Stations on 27 August and 27 September 2012.

All measurements where performed with both irradiance and radiance RAMSES sensors under the ice as well as an irradiance RAMSES sensor on the surface recording the incoming irradiance.

Measurements were either conducted in a half circle around the hole, starting -90° left and ending 90° right of the operator facing towards the sun (if discernable) or under very thin ice the sensor was moved away from the operator until the length of the arm was reached. Special features were noted.

Bio optical cores were taken at the middle position. In some cases this measurement was repeated as last.

On ice station #2 and Heli ice station #2 Spectral Albedos were measured on the site with the ASD Fieldspec

On Ice station #4 samples for optical lab measurements (Scattering) were taken from the access hole.

Times are given in UTC as read from the recording Trios notebook.

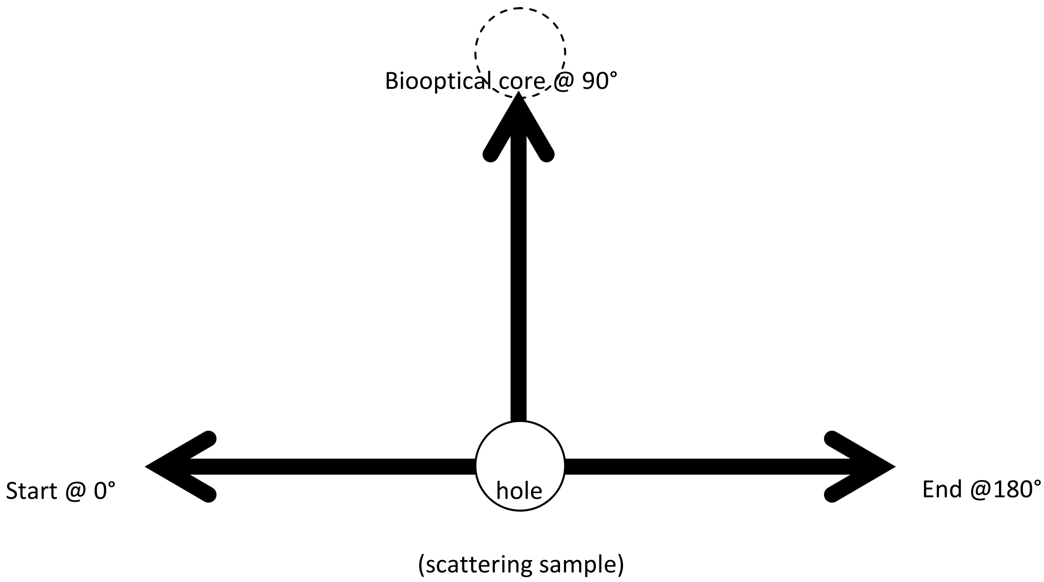

ICE STATION #4 – 26TH AUGUST 2012

MSDA_XE Database of this day is corrupt. Albedo measurements by Larysa on all sites

SITE #1

- White ice
- Scattering core 1 (Sample 8)
- OPT-Core

z_i= 85 cm
z_{surf}= 6 cm
z_s= 0 cm
fb= 17 cm

Irradiance:
first: 4:37:52
last: 4:41:53 (Bio-Core)

Radiance:
first: 4:50:08
last: 4:53:08 (Bio-Core)

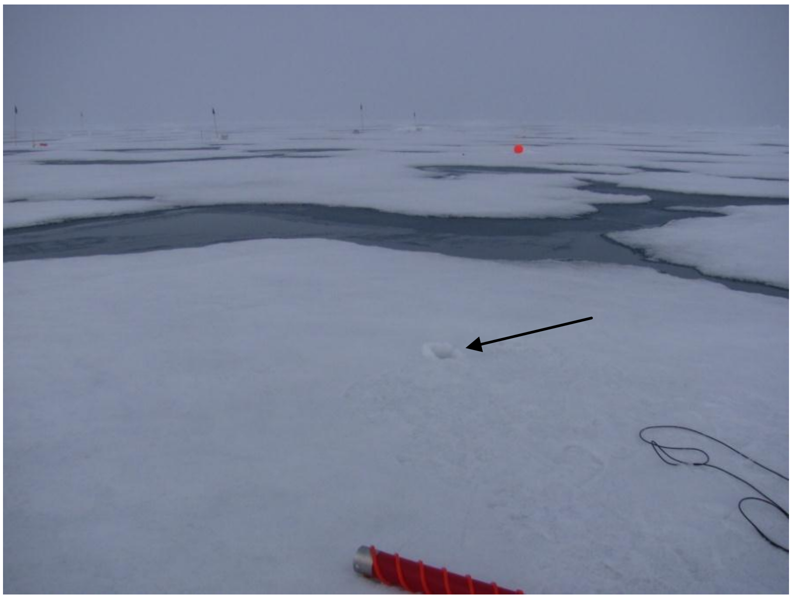

SITE #2

- Melt pond
- OPT-Core

z_i= 31 cm
z_{surf}= 0 cm
z_s= 0 cm
fb= -27 cm

Irradiance:
first: 5:04:14
last: 5:06:35 (Bio-Core)

Radiance:
first: 4:58:51
last: 5:01:51 (Bio-Core)

SITE #3

- white Ice
- OPT-Core
- Scattering core 1 (Sample 9)

z_i= 95 cm
z_{surf}= 0 cm
z_s= 6 cm
fb= 14 cm

Irradiance:
first: 6:46:39
last: 6:49:46 (Bio-Core)

Radiance:
first: 6:51:50
last: 6:54:46 (Bio-Core)

Depth Profile:

RAMSES sensor taped vertically to the cable with the help of a cable-tie

Start:	11:12:20
bottom @ 47m:	11:20:40
top:	11:25:40

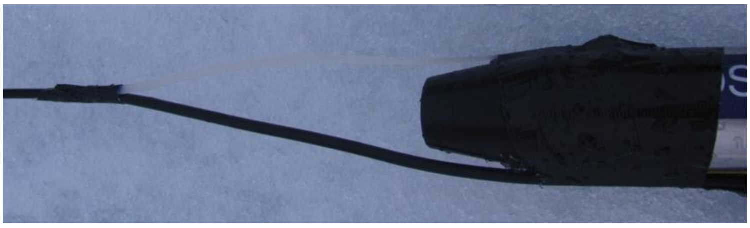

SITE #4

- pond
- OPT-Core

z_i= 35 cm
z_{surf}= 0 cm
z_s= 0 cm
fb= -25 cm

Irradiance:
first: 7:09:40
until 7:10:56 20 cm ice block
last: 7:12:54 (Bio-Core)

Radiance:
first: 7:01:36
until 7:02:31 20 cm lower
last: 7:04:16 (Bio-Core)

SITE #5

- light blue pond
- OPT-Core

z_i=	106 cm
z_{surf}=	0 cm
z_s=	0 cm
fb=	-46 cm

Irradiance:

first:	8:34:19
from	8:35:31
to	8:35:47 deeper
last:	8:37:00 (Bio-Core)

Radiance:

first:	8:41:36
from	8:42:12
to	8:43:01 deeper
last:	8:43:32 (Bio-Core)

HELICOPTER ICE STATION #1 – 27TH AUGUST 2012

MSDA_XE Database of this day is corrupt. No Albedo measurements

SITE #1

- White ice peninsula
-measurements under thin nilas with stretched L-Arm

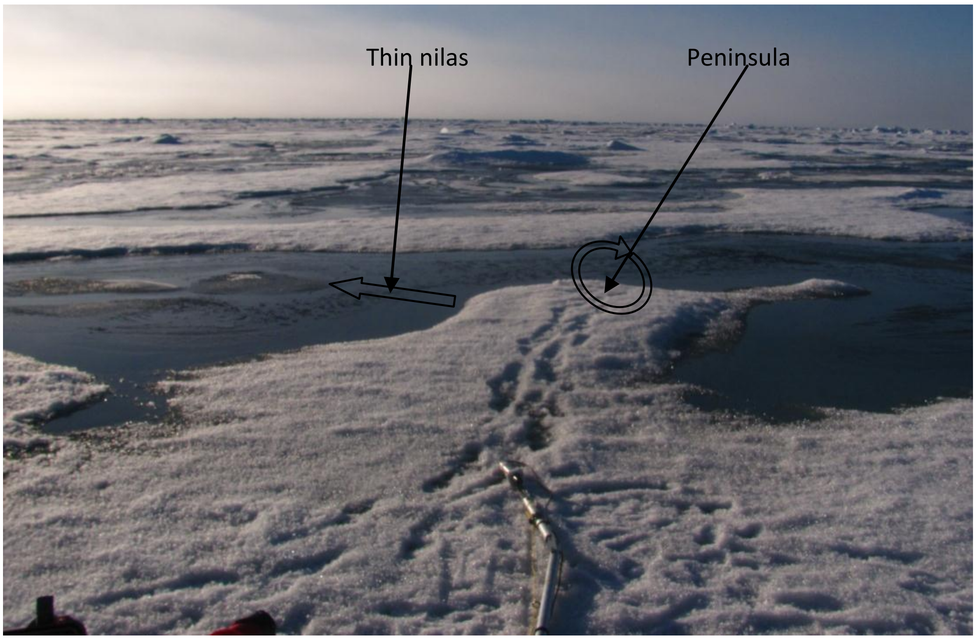

@peninsula:

z_i= 35 cm
z_{surf}= 3 cm
z_s= 0 cm
fb= 5 cm

Irradiance:
first: total first
last: 8:20:50

Radiance:
first: 8:36:20
last: 8:29:37

@thin nilas

Irradiance:
first: 8:28:23
last: 8:29:37

Radiance:
first: 8:43:59
last: 8:45:01

SITE #2 - TRANSECT

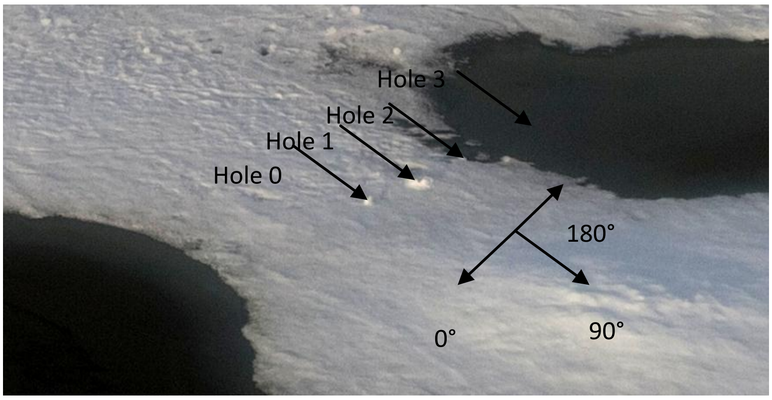

- Transect from white ice to pond
-depth profile in hole 1

<u>hole 0 on white ice:</u>

no optics

z_i= 66 cm; z_{surf}= 3 cm
z_s= 0 cm; fb= 7 cm

<u>hole 1 on white ice:</u>

z_i=70 cm; z_{surf}=3 cm; z_s=0 cm; fb=6 cm

Irradiance:
first: 9:04:00 @0°
45°,90°,135°
last: 9:04:53 @180°
Radiance:
first: 9:08:00 @0°
45°,90°,135°
last: 9:09:16 @180°

depth profile

<u>hole 2 on pond edge:</u>

z_i=50 cm; z_{surf}=0 cm; z_s=0 cm; fb=-13 cm

Irradiance:
first: 9:14:07 @0°
45°,90°,135°
last: 9:14:52 @180°
Radiance:
first: 9:18:00 @0°
45°,90°,135°
last: 9:19:04 @180°

<u>hole 3 in pond:</u>

open pond in 135° position
z_i= 20 cm; z_{surf}= 0 cm; z_s= 0 cm; fb= -28 cm

Irradiance:
first: 9:26:17 @0° (2x)
45°,90°,135°
last: very last @180°
Radiance:
first: 9:23:01 @0°
45°,90°,135°
last: 9:23:41 @180°

HELICOPTER ICE STATION #2 – 27TH SEPTEMBER 2012

SITE #1

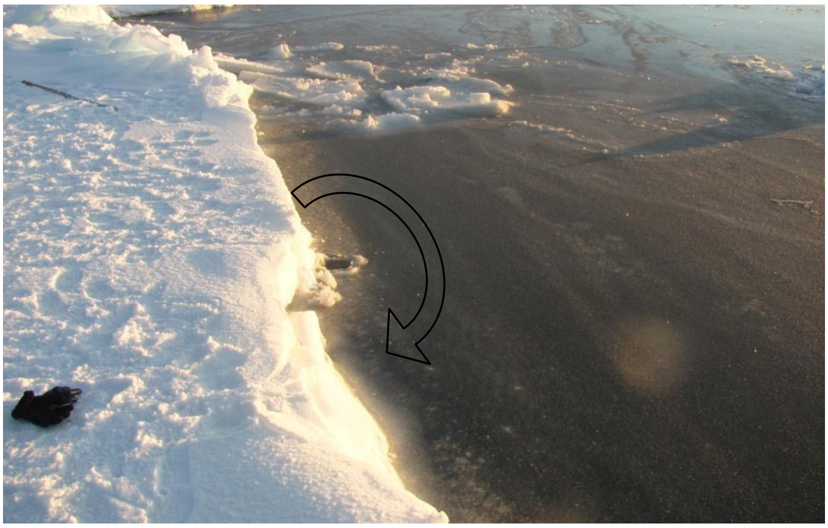

-lead next to small Multiyear floe
-measurements under thin nilas with L-Arm
-Biooptical sample (30x30cm)

z_i= 5 cm
z_{surf}= 1 cm
z_s= 0 cm

Irradiance:
first 0°: 8:54:31
90°: 8:57:46
last 180°: 8:58:49

Radiance:
first 0°: 9:03:57
90°: 9:04:59
last 180°: 9:05:48

SITE #2

-lead next to small Multiyear floe
-measurements under thin nilas with stretched L-Arm
-Biooptical sample (40x20cm)

z_i= 6 cm
z_{surf}= 0 cm
z_s= 0 cm

Irradiance:
first: 9:36:26
last: 9:37:57

Radiance:
first: 9:30:35
last: 9:32:13

SITE #3

-lead next to small Multiyear floe
-measurements under thin nilas with L-Arm
-open water/very thin ice in crack
-Biooptical sample (20x30cm)

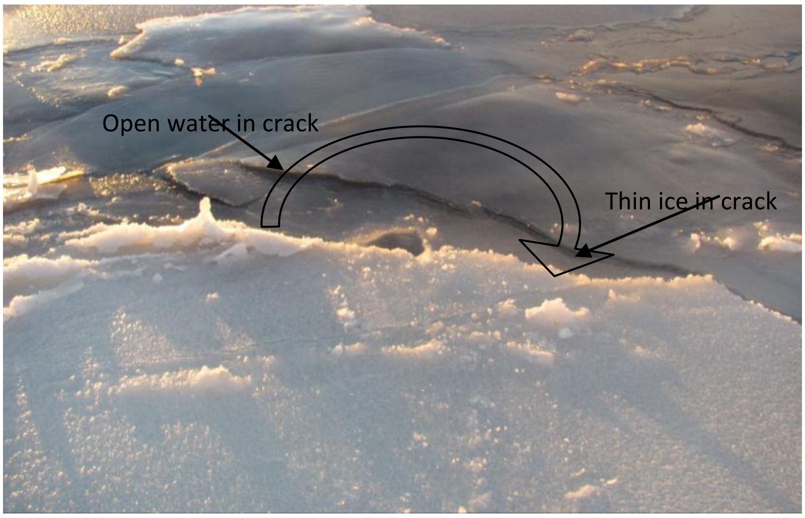

z_i= 4-5 cm
z_{surf}= 0 cm
z_s= 0 cm

Irradiance:
first: 10:27:10
crack : 10:27:35
thin ice: 10:28:48
last: 10:29:14

Radiance:
first: 10:34:43
crack : 10:35:17
thin ice:10:36:25
last: 10:36:37

LONG-TERM-RADIATION-STATION

During Ice-Station #1 we deployed a long-term radiation station on the Ice floe.

SETUP

To determine a safe position, where the ice floe would not drift out or melt within 6 weeks, floe movement was calculated using drift vectors from the last 10 years. As we expected a new minimum in sea-ice extent, we chose a position at 84°N 31°E. The ice floe was chosen by helicopter, looking for the most solid ice-floe in the area. Due to the ice conditions it was difficult to find such a floe due to the strong melting. Finally we picked a thick floe of first-year sea-ice which seemed rigid enough due to a massive ridge with impressive rafting structures and a sail height exceeding 3m. We chose the site for our radiation station in the middle of the floe on a smooth patch of first-year-ice with some well developed ponds. The surface was drained without snow layer and the very first thin ice sheet (<5mm) was forming on the melt ponds. This part of the floe did not show any structural weak parts, while being surrounded of several features with higher possibility of breakup. By this we could hope for sufficient protection of this part of the floe against breakup or compression.

The station was set-up first on the 9. August containing four optical RAMSES-Sensors, the automatic weather station and a Tribox logging-unit with power supply by solar panel and wind generator. The optical sensors were deployed through 9cm corer holes. They were mounted using stainless steel wire hanging from another tensioned horizontal wire to minimize shadowing effects. They were mounted a few decimeters below the sea ice, to increase the sensor footprint reducing disturbance by the hole and avoiding the sensor from icing during freeze-up. Thicknesses of ice and scattering layer were recorded and cores for biological analysis taken.

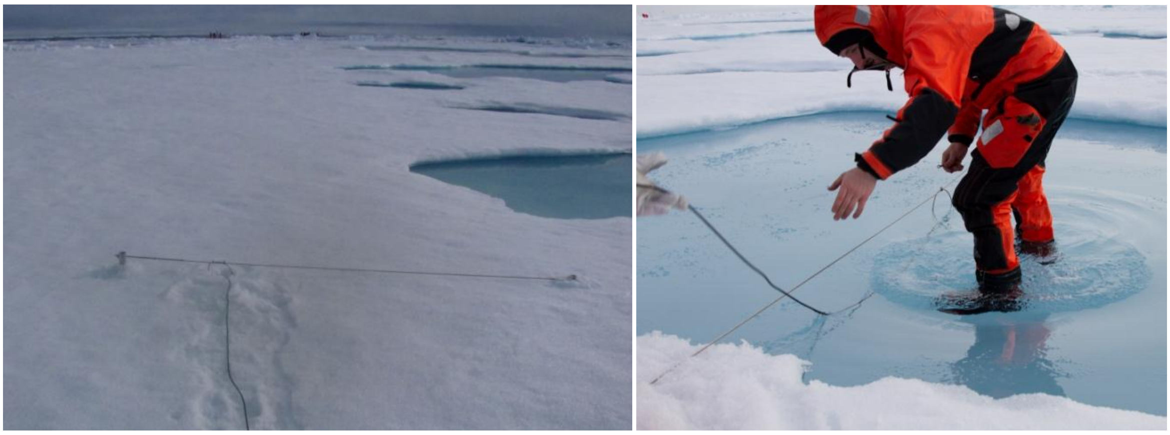

Figure 12: left: Deployment of the under-ice sensor hanging from a horizontally tightened wire. Right: Deployment of the under-pond sensor hanging from a horizontally tightened wire in the melt pond. First frazil ice crystals are visible on the water surface.

On the following days we conducted ROV-surveys on the floe, also passing by the site of the radiation station to measure transmittance and take images of sensor position. Tests of the radiation station revealed, that the Tribox-logging-unit did not work. Due to that, the radiation station had to be rearranged on the last day. We unmounted the Tribox-logging-unit including wind-generator and solar-panel and exchanged it by the *TriOs DSP* datalogger (TriOs GmbH, Rastede, Germany). During testing the sensor mounted under the pond did not work. As time was limited and the albedo-measurement already included in the sensors of the weather station, we moved the reflected sensor under the pond. After all we conducted a successful test run using three optical sensors before leaving it in the afternoon of the 11th august. Battery limitations of the logger were unknown.

The automatic weather station was programmed on board and recorded wind speed, wind direction, air temperature, relative humidity and short-wave as well as long-wave incoming and reflected radiation using a CNR1 albedometer (Kipp & Zonen, Delft, Netherlands). Data was recorded on a CR1000 datalogger (Campbell Scientific, Logan, USA). Data acquisition was successfully tested on the floe during deployment.

ADDITIONAL SENSORS

In addition to the radiation station different additional sensors were deployed at the site. An overview is provided by the following figure. For continuous records of ice and snow thickness, a SAMS-type Ice mass balance buoy was deployed next to the radiation station in cooperation with the biogeochemistry group (Wenzhöfer/ Glud). They also deployed a current meter on the site. A game camera (Trophy Cam, Bushnell, USA) recorded pictures of the measurement site each hour and on IR-movement detection to capture trespassing polar bears.

To ease recovery, the site was marked using 3 about 3m high black flags, a yellow painted radar reflector on the camera mast and a SVP (Surface Velocity Profiler buoy) transmitting position, buoy temperature and air pressure.

As further equipment one SAMS-type IMB together with a sediment trap was deployed on the floe. The big ridge was marked using about ten big black flags, a red painted radar-reflector and a second SVP. The different buoy positions enabled us to track all components of the floe after a possible breakup and as long the floe is still intact a reconstruction of true compass heading of the radiation station by the GPS data.

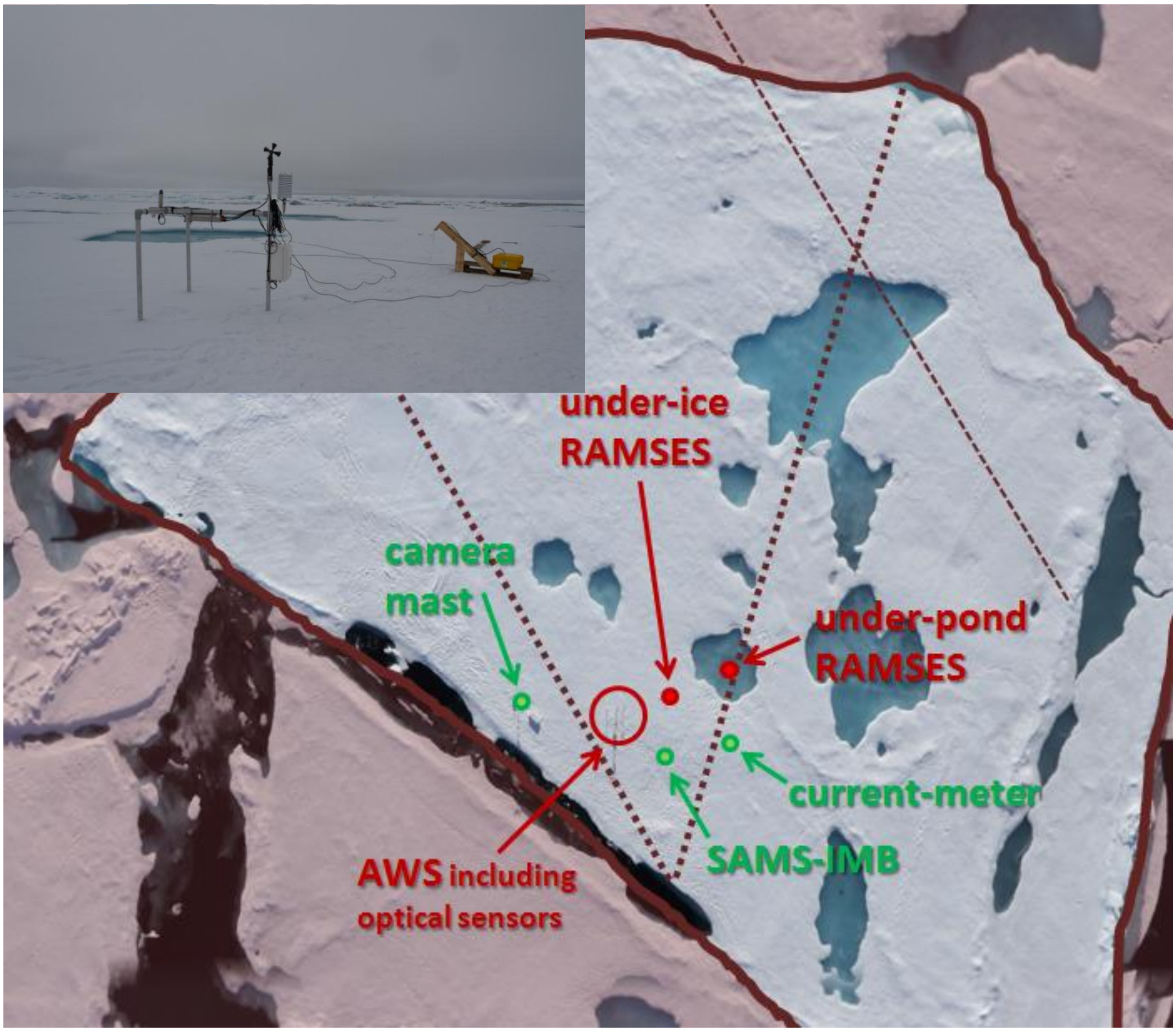

Figure 13: Aerial image of the deployment site of the long-term station shortly after deployment. Locations of the under-ice optical sensors are given by the red dots. The red circle marks the position of all surface sensors of the radiation and weather station. Positions of additional sensors are shown by green dots. Dotted lines show ROV-profile lines before retrieval, while the dashed line indicates the ROV-profile line right after setup. The red shaded areas broke away from the floe during the observation time, whereas the unshaded central area was found unchanged during retrieval.
Inlay: Picture of the radiation Station after setup. The IMB is the yellow PELI case visible to the right.

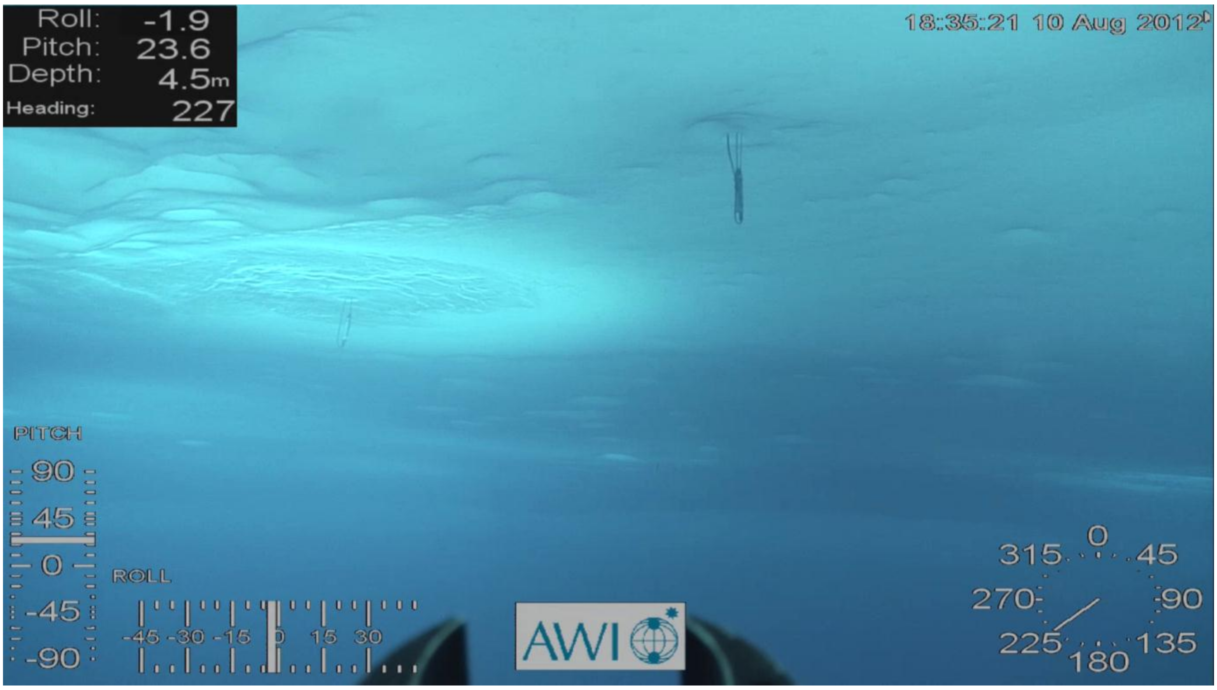

Figure 14: Under-ice image taken by the ROV of the survey site. The floe consists of even level ice. Both under-ice RAMSES sensors are visible. While the front one is hanging under uninfluenced bare ice, the increased light transmittance under the pond is clearly visible, with the sensor positioned under the brightest spot.

OBSERVATIONS

After deployment, we received the positions of the SVP buoys each hour directly onboard *Polarstern*. That enabled us to keep track of the floe movement and to relocate it for retrieval. The floe was first drifting southward with a high speed towards the ice edge but turned west around 83.6°N. In the end of august the regional drift-pattern changed due to southerly winds and the floe turned northward. On the 1st September around 20^{00} there is the first substantial change in the distance between both SVPs increasing from the initial 80 m to about 120m. The breakup can be linked to the passage of a low pressure system in the area. As both buoys were found in the same position relative to their surrounding on retrieval, this can be associated to a first breakup of some parts of the floe. On the 6th September around 17^{00} the floe finally breaks up and the two parts drift separately with a distance between 400 m and 1000 m. In calm conditions and cold temperatures on 22nd September the distance between both buoys gets stationary again indicating that the whole surroundings consolidate by freeze up forming new ice and a new bigger ice floe.

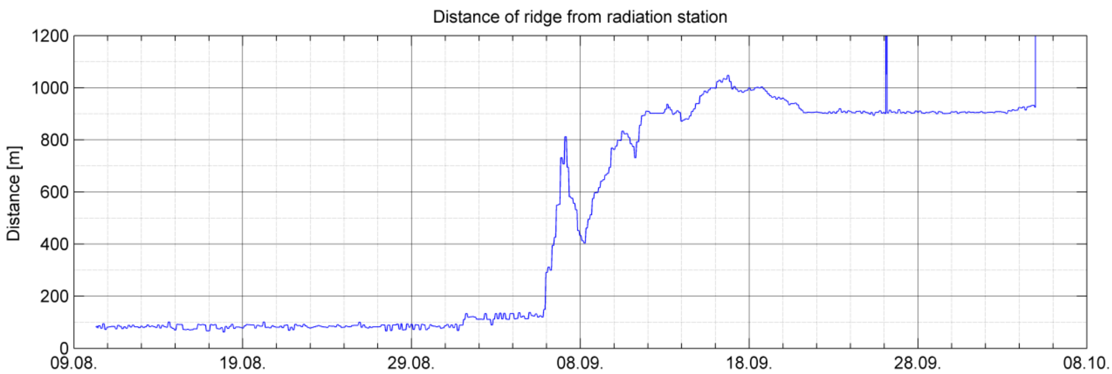

Figure 15: Time series of the distance between the SVPs located at the radiation station and the large ridge. Except of some GPS-data scatter the distance keeps constant befor the first September and after the 22nd September.

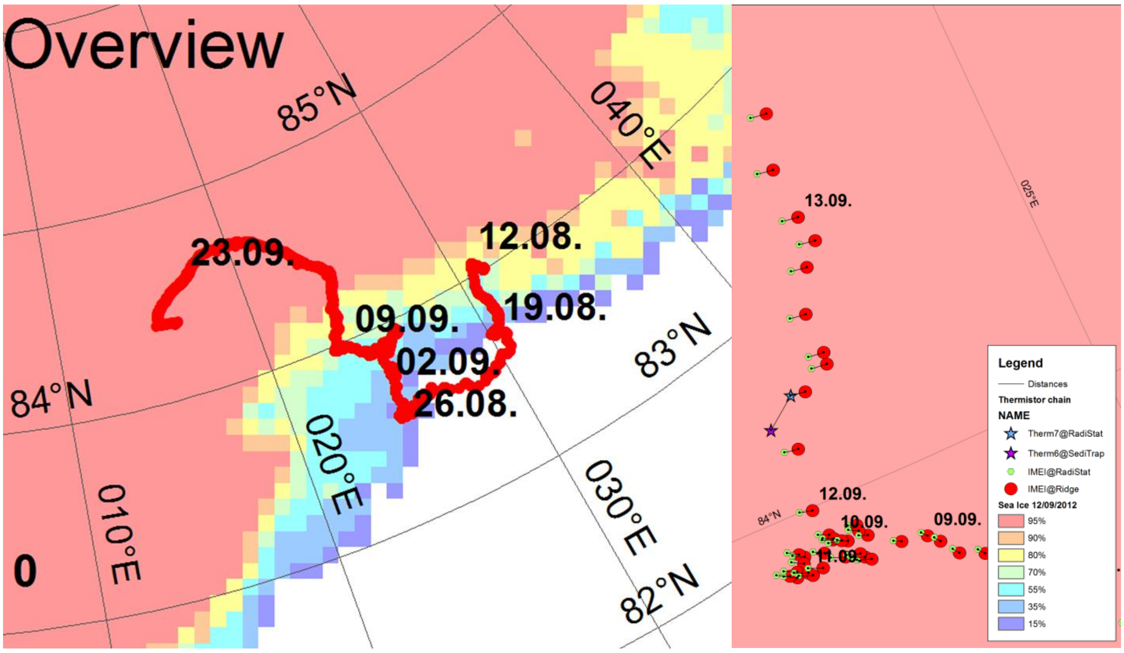

Figure 16: Drift track of the long-term-station during its whole drift (left) and detailed drift track of different buoys shortly after floe breakup.

All buoys deposited on the long-term station are listed in the following table. SVP data were delivered via mail directly to the ship and SAMS-IMB data can be accessed via http://martech.sams.ac.uk/ronnie/

Location	Type	IMEI
marked ridge	SVP	300234010080670
camera mast	SVP	300234010086650
radiation station	SAMS-IMB	300234010899710
sediment trap	SAMS-IMB	300234011178960

Figure 17: On 9th September 11:30 (UTC), the station got visited by an interested polar bear. He stepped over the flag visible in the right and ripped the cable of the temperature and humidity sensor. The picture taken by the automated camera shows well the changed surface conditions, though the pond is still visible to the left as a depression in the snow surface. The camera stopped working ten days before retrieval.

The recorded weather data is shown in the following figures. Air temperature can be inferred from the SVP hull temperature after failure of the Humidity and Temperature sensor. Albedo values (blue curve) range between 0 and 1.5 after taking into account, that the albedometer was maybe mounted or connected upside-down. The wind sensor was standing still due to strong icing at retrieval, indicating that it has not been working since the 18th September. No preferential wind direction was found in the data.

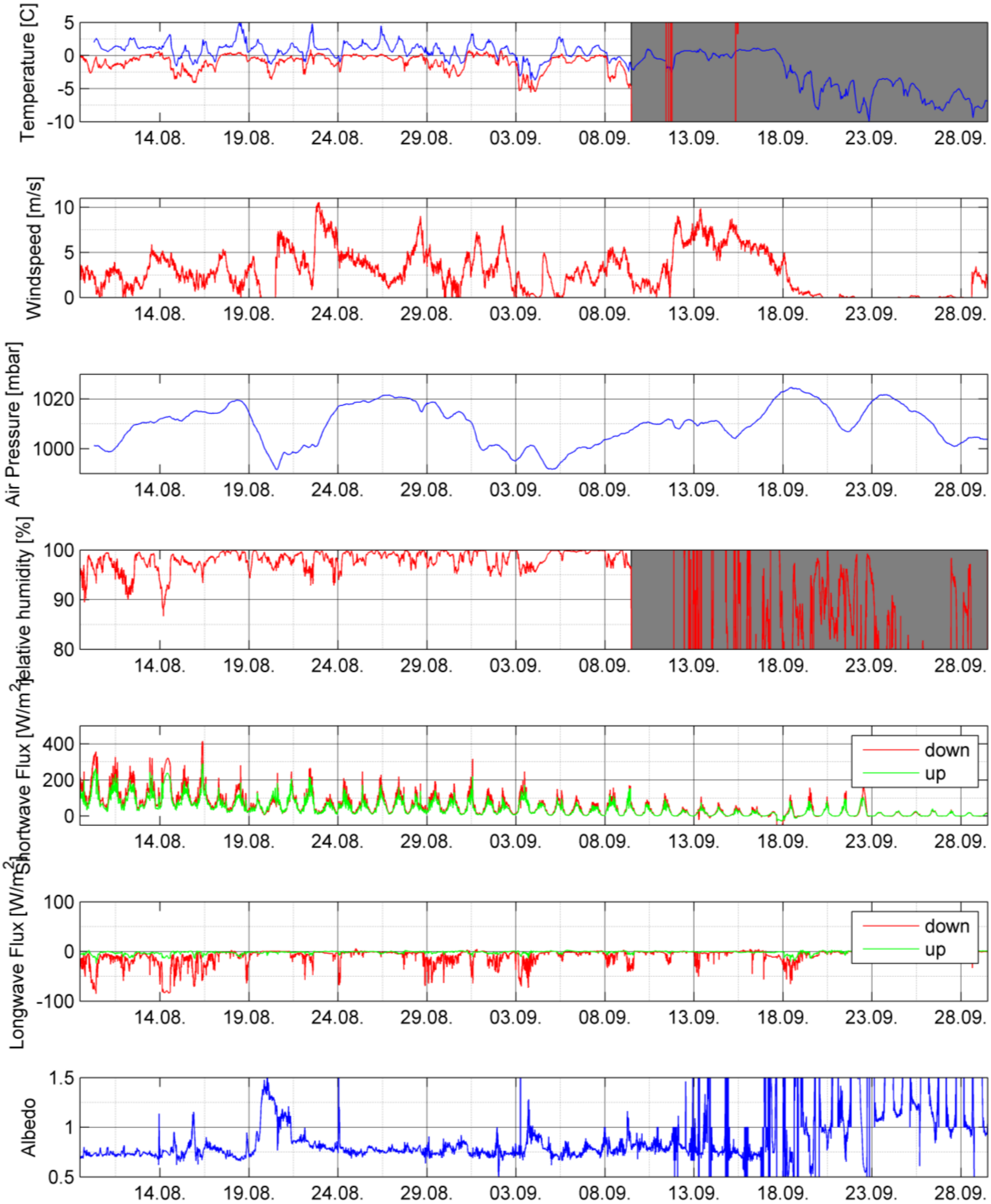

Figure 18: Data from the automated weather station. A) Air temperature (red) and SVP hull temperature, gray shading marks the damaged temperature sensor B) Windspeed registered at the AWS. Due to strong icing, values after 20th September are unreliable C) Air pressure measured by the SVP D) relative humidity, gray shading marks the damaged sensor E) Up- and downwelling shortwave fluxes F) Up- and downwelling longwave fluxes G) Shortwave albedo (blue).

We measured (uncalibrated) transmittances of ~2% for the bare-ice case. Bare-ice transmittance did not vary much throughout the observation period, as the surface properties did not change much, though snowfall events are clearly reducing the transmittance of the bare-ice.Transmittance valuesof ponded sea-ice were around 15% until the first snow on 19th august. After a sharp decrease to 10% they kept variable in the range between 10% and 15% depending on the snow conditions. On 4th September a strong snowdrift started filling up the ponds with snow, reducing the transmittance to a minimum of 1%. Afterwards transmittance increased again due to surface degradation and sublimation of the snow and rime covering the pond surface. A second drop occurred on the 18th September during a temperature drop with icing conditions. This temperature drop seems to be the reason for the failure of the automatic camera

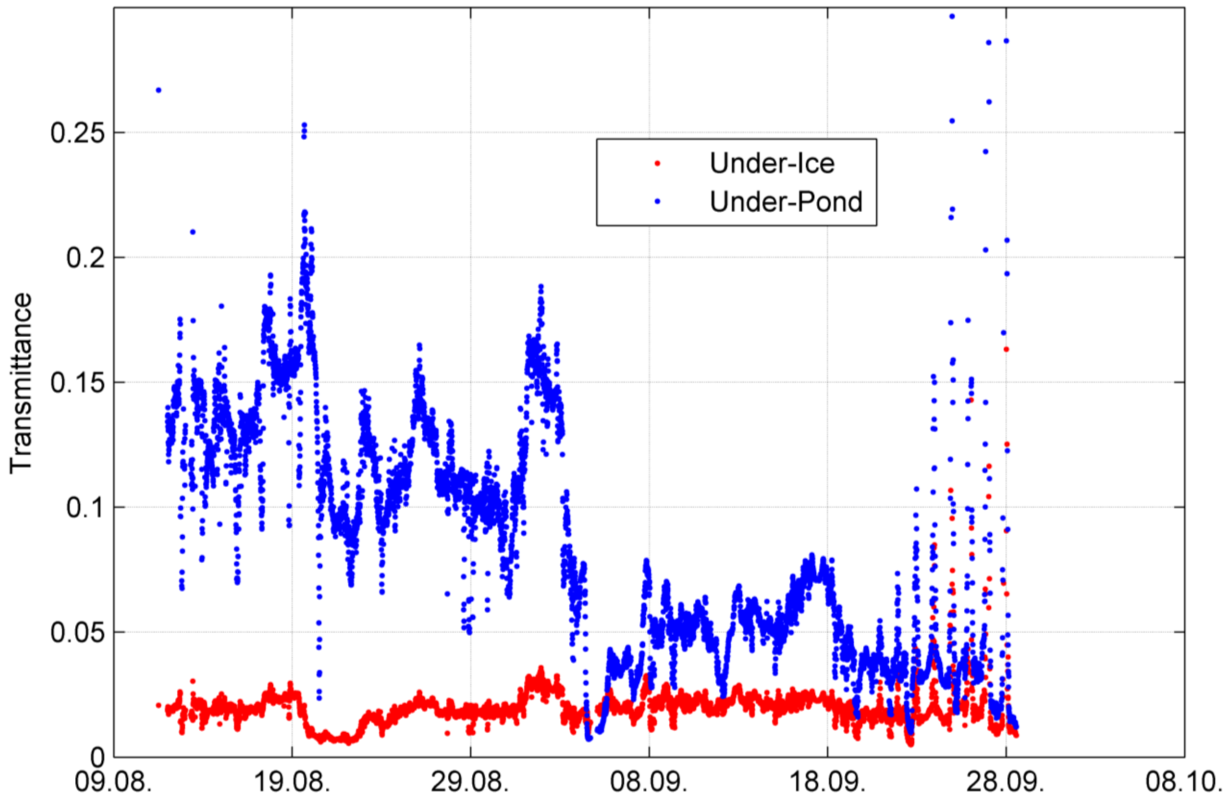

Figure 19: Data from the automated weather station. A) Air temperature (red) and SVP hull temperature, gray shading marks the damaged temperature sensor B) Windspeed registered at the AWS. Due to strong icing, values after 20th September are unreliable C) Air pressure measured by the SVP D) relative humidity, gray shading marks the damaged sensor E) Up- and downwelling shortwave fluxes F) Up- and downwelling longwave fluxes G) Shortwave albedo (blue).

RETRIEVAL

On 28th September we approached the long-term site, using the most recent buoy positions in combination with a drift estimate as waypoint. By this means it was relatively straight forward to find the well marked ridge site. Even though the floe had broken up in several parts, it was easy to locate the radiation station about one km further away. Good sight and light conditions enabled this fast search. To reduce influence on the measuring site and to speed up operations, the ship stayed at the floe edge a few hundred meters away from the station. The station was approached by snow mobile. It was found in a good shape, though several sensors were influenced by icing. The TriOs datalogger was retrieved immediately, and analysed on board, while the rest of the station was left untouched until the next morning. All data loggers successfully recorded data during the whole installation time, only the automated camera had failed some days before retrieval.

Figure 20: Images of the long-term installations before retrieval. SAMS-IMB (top left), the pressure ridge marked with flags and SVP (top right) and the weather and radiation station after retrieval of the datalogger (bottom).

SENSOR CONDITIONS

The radiation station was found intact and without any recognizable tilt. The height of the middle of the main bar above the snow surface was 95 cm. The downward pointed sensor of the albedometer was 80cm above the snow surface. The Photometers were covered by icing, while the measurement surface of the RAMSES was free and icing had only built up on the sensor's side.

Before retrieval the under-ice sensors were photographed with the ROV, while the sensor positioned under the bare ice was hanging as supposed, the under-pond sensor was hanging with an inclination of approximately 45° due to tension in the sensor cable. It is unsure, whether this tilt occurred during setup when changing the sensor configuration in the last minute or if the support wires melted into the surface and lost tension. This was unfortunately not observable from the inclination value given by the RAMSES sensor itself as this specific sensor did not contain an IP-module.

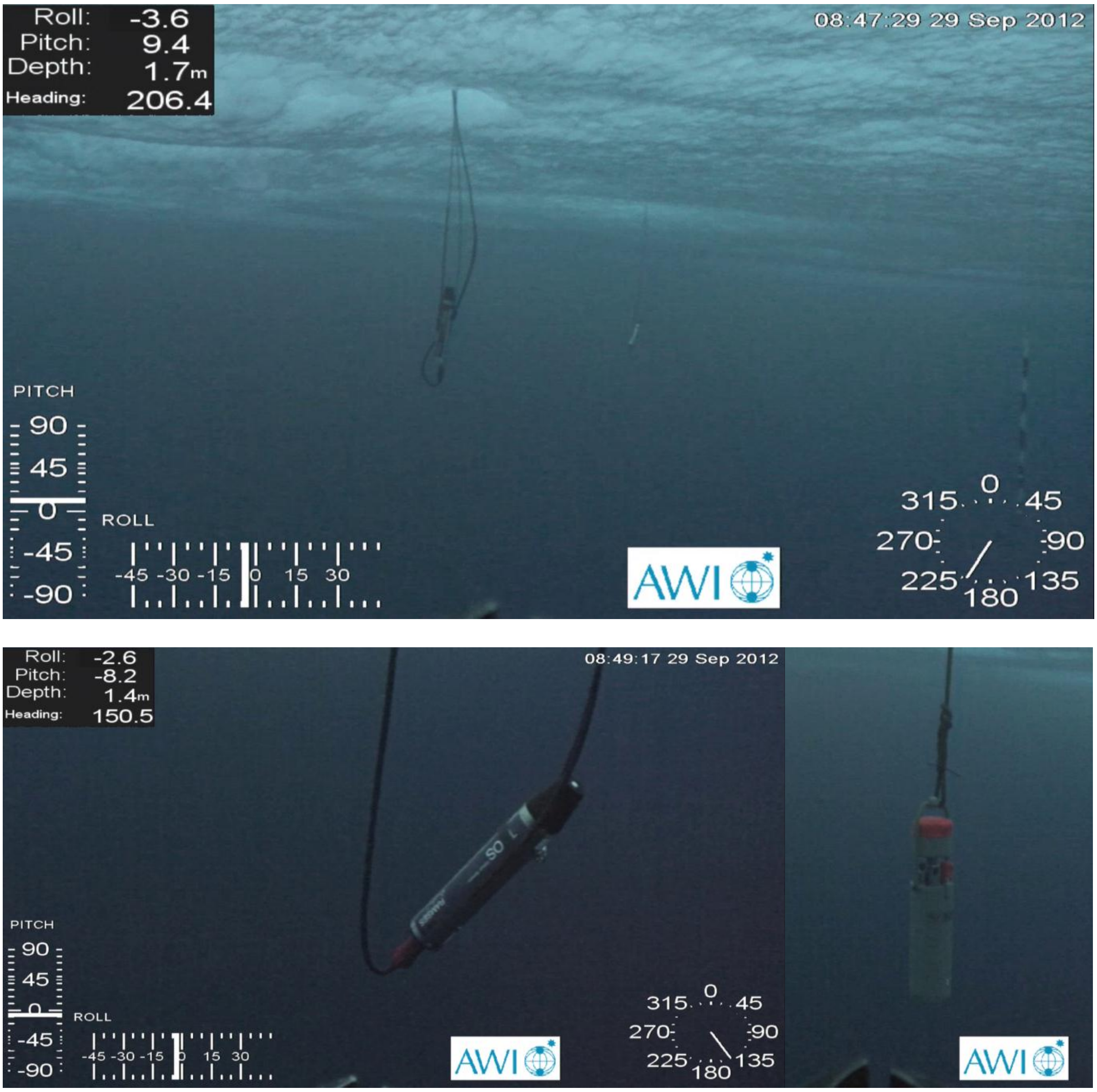

Figure 21: Images of the under-ice sensors taken by the ROV on 29th September. The upper picture shows both sensors from a similar viewpoint as in figure XXX. The under-pond sensor (bottom left) was hanging with an inclination of approx. 45°. The current meter is shown in the bottom right image.

Sensors were located by drilling a hole close to the sensors, while the ROV pilot was observing from underneath, directing the drillings until close to the sensor. Then sensors were retrieved using ice-saws, ice-axes and ice-corers. All wires and cables were cut and partly left behind, as it was impossible to retrieve them.

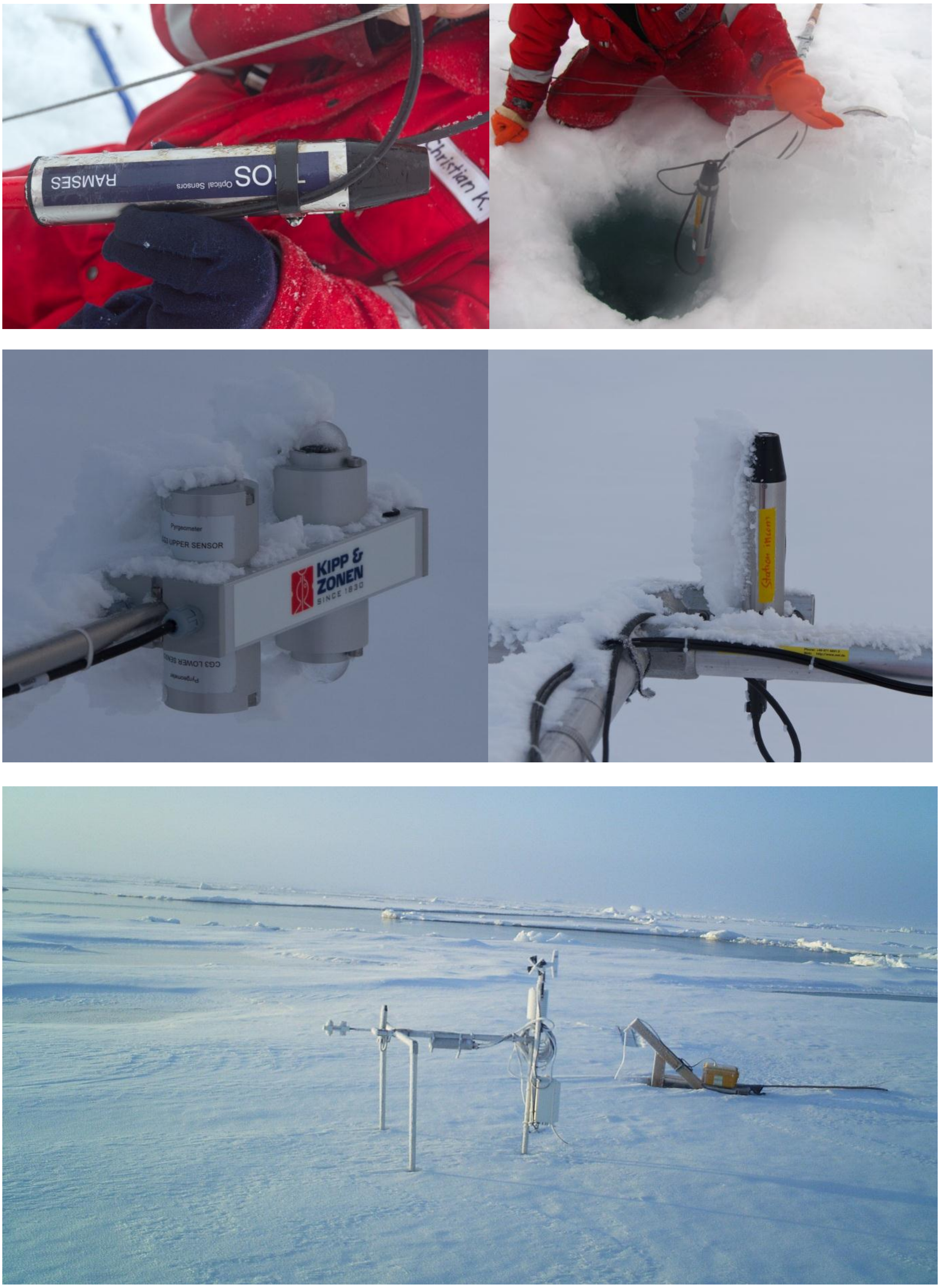

Figure 23: Algae cover growing on the upper side of the under-pond sensor is visibleafter retrieval (top left). Retrieval of under-ice sensor (top right). Albedometer before retrieval covered in rime (middle left). Surface RAMSES sensor before retrieval (middle right). Last picture taken by the automatic camera on 18th September (9:30 UTC) 10 days before pickup.

ALGAE GROWTH ON SENSORS

During retrieval, we observed a brown layer of algae on the upward facing side of the RAMSES-sensor which was hanging under the melt pond. Some of the loosely attached Algae were scraped off by hand and analysed with a microscope onboard the ship. They consisted of typical sea ice algae, so mainly pennate diatoms (Nitzschia sp. and Navicula sp.). The small sizes indicate recent development. They were found in a good shape, so they were probably photosynthetically active. No algae-growth was observed on the sensor located under bare ice.

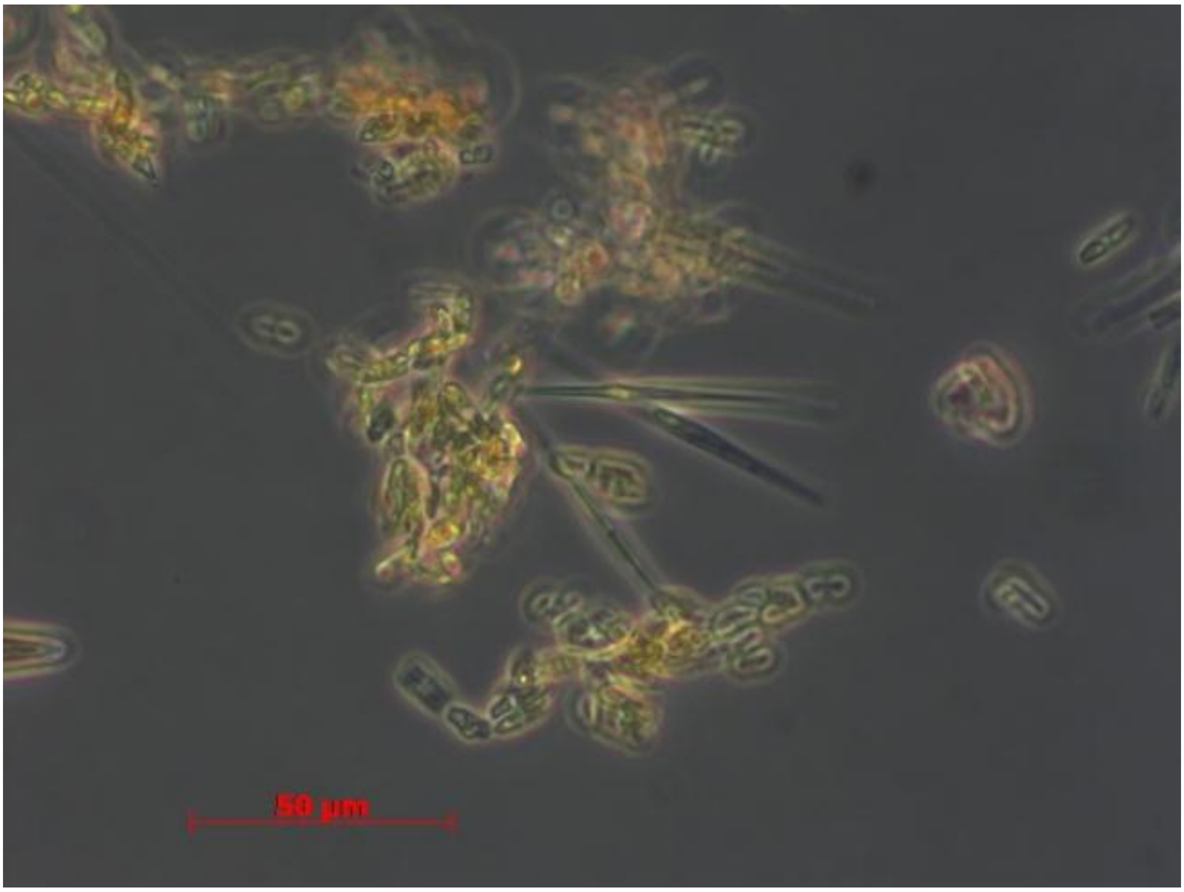

Figure 24: Photographs of the sea-ice diatoms growing on the sensor placed underneath the melt pond. The small sizes indicate recent growth. Pictures were taken using an inverted light microscope with phase contrast optics (Axiovert 40C Zeiss Germany) and an integrated camera (AxioCam MRc Zeiss Germany). Picture: Mar Fernández/Christian Katlein

SNOW AND ICE GEOMETRY

Snow and ice geometry was measured at the sensor sites during sensor setup and retrieval. During retrieval the optical cores were taken in the close vicinity of the sensors. This is the reason for slight deviations between measurements during retrieval.

Location	Time	z_Ice [cm]	z_Snow [cm]	fb [cm]	scattering layer [cm]	z_s+surf [cm]
under ice sensor	Setup OPT	170	0	28	5	5
under ice sensor	retrieval	143	-	27	-	16
under ice sensor	retrieval OPT	156	3	28	0	3
pond sensor	Setup OPT	111	0	-26	0	0
pond sensor	retrieval	107	-	2	-	2
pond sensor	retrieval OPT	113	6	3	0	6

SNOW VARIABILITY

To assess the spatial variability of the snow cover around the measuring site, we obtained a snow grid. Snow thickness was measured using a marked wooden stick (Tuchelle) with a cross section of 1x1 cm. The albedometer of the radiation station was mounted in position (x=1,y=10), while the coordinates of (x=10,y=10) and (x=10,y=1) were located at the ROV-profile markers M3 and M5 respectively.
Snow measurements along the profile and the at coring sites were measured using pointed metal sticks (Ø ca. 5mm, marking flag) and differ from these measurements. While the snow thickness under the Albedometer measured with the wooden stick was 3cm, a measurement with the metal flags gave a measurement of 10cm.

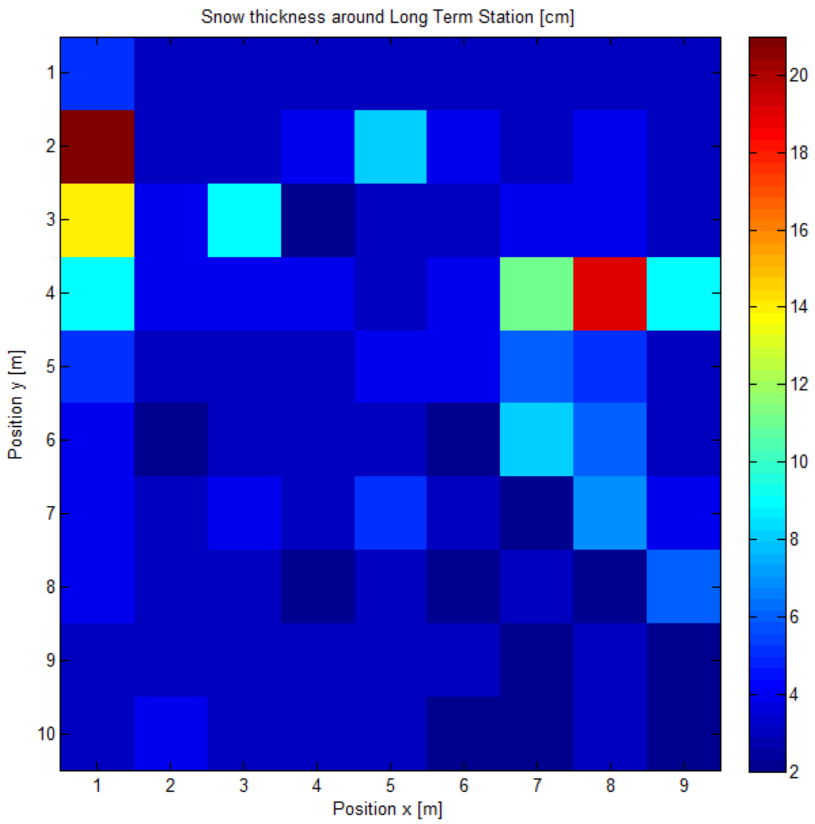

Figure 25: Grid measurements of snow at the long-term observation site. The albedometer was located in the lower left corner. The right edge is described by the ROV-profile, with marker M3 in the lower and M5 in the upper corner.

ALBEDO-OBSERVATIONS

Spectral short-wave-albedo was measured on various sites on each ice-station, several helicopter-stations, as well as along the ROV-transects with an ASD Field Spec.

Albedo-Data will be included in the processing of ROV-Data and published in the PANGAEA-database.

Figure 26: Albedo-measurements along the ROV-transect

RADIATION MEASUREMENTS ON CROWNEST

During the whole cruise, we operated one RAMSES Irradiance sensor in the ship's crownest. The sensor was inspected few times during the cruise, but showed substantial icing only in one case. Data was normally recorded in a five minute interval, but during SUIT-trawls the sampling frequency was reduced to five seconds. This data will be used for validation of the RAMSES sensors against the ship's photometers and to compare with the reference sensor on the ice-floe.

ICE-CORING AND FURTHER SAMPLING

Ice cores were taken at the main and secondary coring site on each station and analysed for various parameters (see official cruise report). Along the ROV-transects several ice cores were retrieved for sediment and biological analysis. A complete list of all sea ice samples taken during the cruise can be obtained on http://doi.pangaea.de/10.1594/PANGAEA.792734. The following labels were used in the database to identify optical measurements:

Label	Description
ALB	Albedo measurement
ROV	Launch hole of ROV
RAMSES	Spectral transmittance measurement
ICES	Ice sample for scattering experiments
CORE_OPT	Bio-optical core
CORE_ARC	Archive core (stored at Fishery harbor, Bremerhaven)
CORE_SAL	Salinity
CORE_TEX	Ice texture
CORE_DEN	Ice density

LAB-EXPERIMENTS

In the case of an isotropic light field readings from a radiance sensor can be converted into irradiance by a multiplication with π. During the data analysis of the TransArc-ROV-data we discovered, that the relationship between readings from the irradiance sensor and the radiance sensor was significantly different from those expectations. Further assessment lead to the definition of the new quantity transflectance. Findings in Katlein (2012) suggest a dependency on anisotropic scattering in the ice and hereby with the lamellar crystal structure of sea-ice.

To increase knowledge about the angular shape of the radiance field under sea-ice we conducted roll-experiments with the ROV (see above). To quantify the influences of different ice types we examined 7 samples in the Ice-Container at -20°C. Samples were retrieved from the lowermost part of the 12cm-diameter core taken close to the ROV tent as access hole for the USBL-Transducer. Cubic samples with a edge length of around 8 cm were cut, and the surfaces sanded and handpolished as described by Grenfell and Hedrick (1983).

Horizontal and vertical extinction coefficients, as well as angular dependence of exiting radiance were measured with the following setup shown in figure 29. All measurements were carried out using two different light sources. A Quante 310D1 (Quante Baulaser GmbH, Wülfrath, Germany) with very good beam characteristics, producing a stable beam (λ = 635 nm) with beam diameter of 6mm and divergence of less than 0.2 mrad was used for collimated illumination. Diffuse illumination was achieved by using a standard 75W OSRAM light bulb behind a glass diffuser plate. Both light sources were positioned as close as possible to the sample table (20cm long, 13.5 cm wide) which was covered in black tape to avoid reflections. The ice samples were positioned at the end of the light table. The samples were put in front of a 5mm thick cardboard mask with a rectangular opening of 7x7 cm to avoid stray light from entering the detector and masking out light rays close to the sample edges. In case of diffuse illumination we used a second mask to avoid illumination through the side of the samples. As detector we used the same type as used during the ROV measurements. A RAMSES-ARC (TriOs, Rastede Germany) was mounted on an arm which could be rotated around the vertical axis going through the middle of the sensor facing side of the ice sample. The sensor was used in two different positions 32.7 cm and 17.5 cm away from the sample surface.

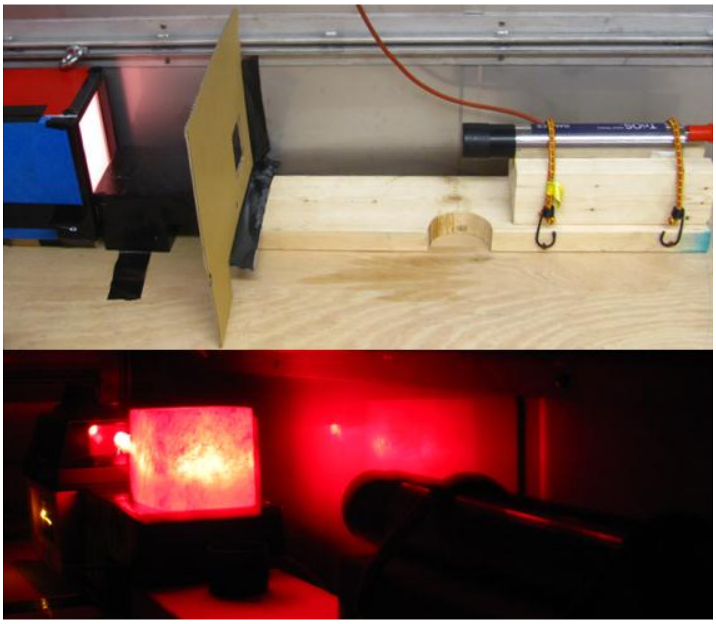

Figure 27: Photographs of the lab setup both in the case of diffuse illumination (upper image) and collimated illumination by laser (lower image). In both cases there is one of the straylight masks missing for better visibility of the setup.

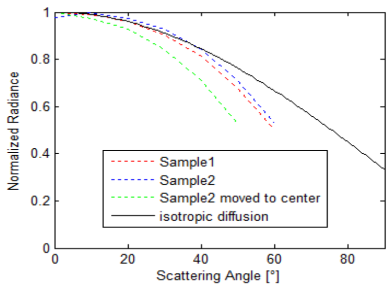

Figure 28: Preliminary results of the angular dependence of exiting radiance showing a clear deviation from the isotropic case.

Extinction was measured in both orientations along the growth- or depth-axis and all four horizontal orientations to determine the anisotropy of extinction. Angular dependence of exiting radiance was measured only in the "natural" orientation with the ice bottom facing towards the sensor. Additionally both light sources were measured during a longer time period of at least one hour after power on, to estimate intensity-drift.

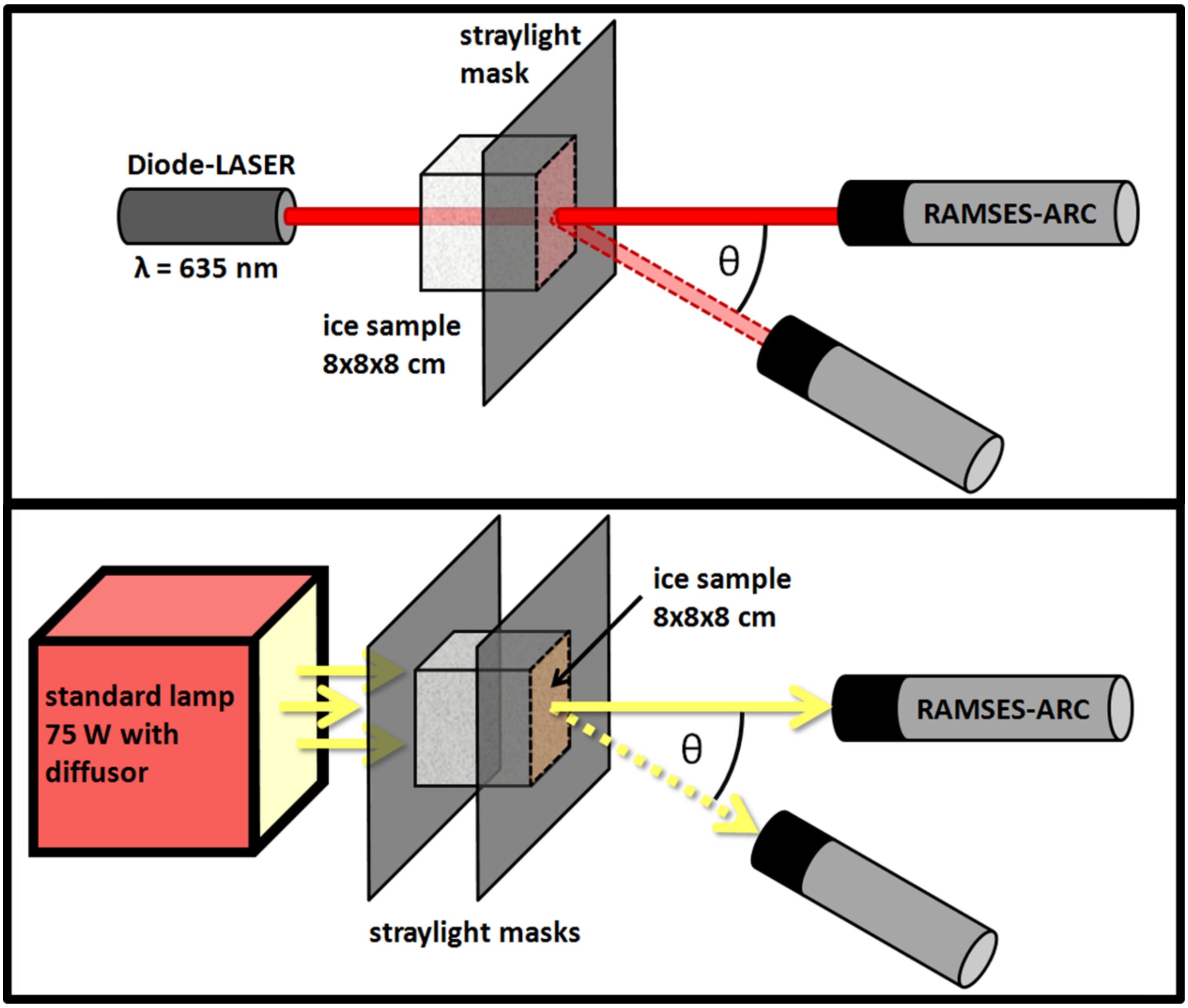

Figure 29: Schematic sketch of the lab setup both in the case of diffuse illumination (upper image) and collimated illumination by laser (lower image). θ denotes the scattering angle.

To analyze the microstructure of the samples, we prepared thin-sections from the ice cuttings, left over from cutting the cylindrical sample into cubical shape. For each sample one horizontal and one vertical thin section were prepared to be able to quantify the amount of anisotropy of the crystal structure to complement interpretation of the optical results. All prepared thin-sections are shown in figure 30. The geometries of all samples were measured using a caliper and their weight determined to ±5g. By these values we were able to calculate bulk density and porosity. Values are given in the following table:

Sample #	Weight (g)	B (cm)	H (cm)	T (cm) vertical axis	bulk density g/cm^3	Porosity %
1	510	8,625	8,62	8,52	0,81	12,5
2	377	8,05	7,84	7,965	0,75	18,5
3	400	7,84	7,83	7,82	0,83	9,4
4	430	7,88	7,79	7,88	0,89	3,4
5	418	7,97	7,89	7,81	0,85	7,5
6	390	7,93	7,925	7,97	0,78	15,4
7	445	7,91	7,92	7,925	0,90	2,6

Sample #	Station #	Date
1	255	21. Aug 12
2	224	10. Aug 12
3	323	05. Sep 12
4	335	08. Sep 12
5	349	19. Sep 12
6	360	22. Sep 12
7	384	29. Sep 12

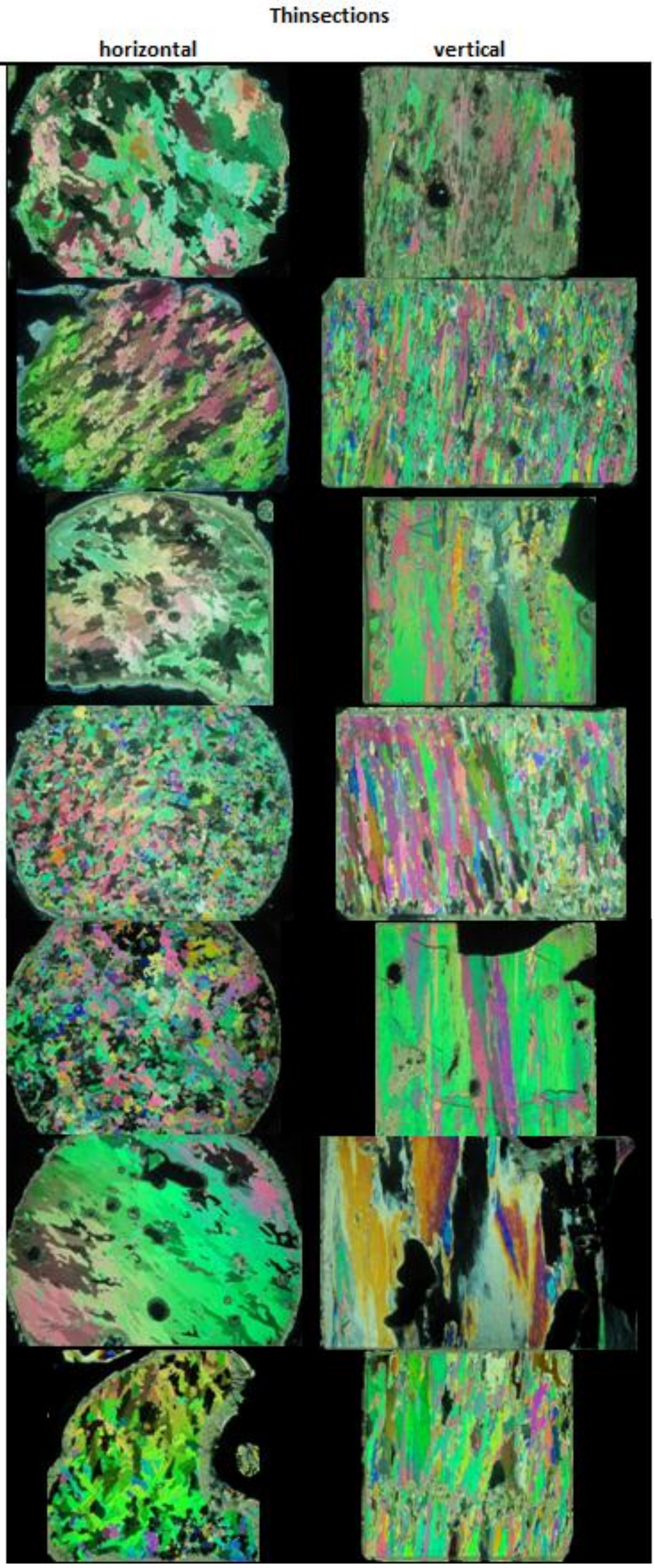

Figure 30: Table showing the prepared thin sections of samples, as well as the date and station number of sampling.

All samples and thin-sections are stored in the ice-core storage of AWI in the fishery harbor Bremerhaven to keep them accessible in the case of needed further examination.

REFERENCES

Boetius, A. (2012). The Expedition of the Research Vessel "Polarstern" to the Arctic in 2012 (ARK-XXVII/3 - IceArc). Berichte zur Polar- und Meeresforschung. Bremerhaven, Alfred-Wegener-Institut.

Fahrbach, E. and R. Knust (2012). Expeditionsprogramm Nr. 89 - FS Polarstern. Bremerhaven, Alfred-Wegener-Institut.

Grenfell, T. C. and D. Hedrick (1983). "Scattering of visible and near infrared radiation by NaCl ice and glacier ice." Cold Regions Science and Technology **8**(2): 119-127.

Katlein, C. (2012). ROV basierte Untersuchung der räumlichen Variabilität der Lichttransmission durch arktisches Meereis im Sommer Diplomarbeit, Eberhard-Karls-Universität Tübingen.

Nicolaus, M. and C. Katlein (2012). "ROV-based measurements of light under sea ice (in preparation)." The Cryosphere Discussion.

Schauer, U. (2012). The expedition ARKTIS-XXVI/3 of the research vessel "Polarstern" in 2011. Bremerhaven, Alfred Wegener Institute for Polar and Marine Research. **579:** 271.